

# Generalized Two-Dimensional Quaternion Principal Component Analysis with Weighting for Color Image Recognition

Zhi-Gang Jia, Zi-Jin Qiu, and Mei-Xiang Zhao

**Abstract**—A generalized two-dimensional quaternion principal component analysis (G2DQPCA) approach with weighting is presented for color image analysis. As a general framework of 2DQPCA, G2DQPCA is flexible to adapt different constraints or requirements by imposing  $L_p$  norms both on the constraint function and the objective function. The gradient operator of quaternion vector functions is redefined by the structure-preserving gradient operator of real vector function. Under the framework of minorization-maximization (MM), an iterative algorithm is developed to obtain the optimal closed-form solution of G2DQPCA. The projection vectors generated by the deflating scheme are required to be orthogonal to each other. A weighting matrix is defined to magnify the effect of main features. The weighted projection bases remain the accuracy of face recognition unchanged or moving in a tight range as the number of features increases. The numerical results based on the real face databases validate that the newly proposed method performs better than the state-of-the-art algorithms.

**Index Terms**—Generalized 2DQPCA; Weighted projection; Color face recognition; Color image reconstruction; Quaternion matrix.

## 1 INTRODUCTION

Two dimensional quaternion principle analysis was proposed to scratch the features of color face images in [1] and had been well developed for the dimensional reduction and the color image reconstruction in [2]–[5]. This contributes to the development of the fundamental tool—the principal component analysis—of deep learning frameworks. The two dimensional quaternion principle analysis based approaches have the advantages at preserving the spatial structure and color information of color images and costing less computational operations. In this paper, we further generalize the two dimensional quaternion principle analysis with utilizing  $L_p$  norms of quaternion vectors to obtain more geometrical and color information and to resist more kinds of noises. We also redefine the gradient operator of quaternion vector functions and present a fast iterative algorithm of feature extraction. Our aim is to present a new generalized two dimensional quaternion principle analysis based approach for color image recognition, which significantly promotes the robustness and the ratio of recognition.

It is well known that two dimensional quaternion principle analysis (2DQPCA) generalizes two dimensional principle analysis (2DPCA) [6] to the quaternion skew-field with a strong motivation of applying the color information of color images. Recall that principal component analysis (PCA) [7] is an unsupervised learning approach for feature extraction

and dimension reduction. It has been widely used in the fields of computer vision and pattern recognition. Recently, many robust PCA (RPCA) algorithms are proposed with improving the quadratic formulation, which renders PCA vulnerable to noises, into  $L_1$ -norm on the objection function, e.g.,  $L_1$ -PCA [8],  $R_1$ -PCA [9], and PCA- $L_1$  [10]. Besides robustness, sparsity is also a desired property. By applying  $L_0$ -norm or  $L_1$ -norm on the constraint function (also called penalty or regularization [11], [12]) of PCA, a series of sparse PCA (SPCA) algorithms [13]–[17], have been proposed. In order to enhance both robustness and sparsity at the same time, robust sparse PCA (RSPCA) is further developed, see [18] and [19] for instance. Considering that  $L_0$ -norm,  $L_1$ -norm and  $L_2$ -norm are all special cases of  $L_p$ -norm, it is natural to replace the  $L_2$ -norm in traditional PCA with arbitrary norm, both on its objective function and constraint function, as proposed in generalized PCA (GPCA) [20], [21].

When being applied to extract feature from images, PCA treats each sample as a vector, and hence, 2D images are converted to high-dimensional vectors prior to feature extraction [7]. To avoid the intensive computation of high-dimensional data, Yang *et al.* [6] proposed the 2DPCA approach, which constructs the covariance matrix by directly using 2D face image matrices. 2DPCA directly constructs the sample covariance matrix from the two-dimensional image, which reduces the burden of calculating the sample covariance matrix from the high-dimensional vectors, and therefore has higher computational efficiency. In addition, 2DPCA processes a two-dimensional matrix to preserve the spatial structure of the images [6], [22], [23], and achieves a higher face recognition rate than PCA in most cases. This image-as-matrix method offers insights for improving above RSPCA, PCA- $L_p$ , GPCA, etc. The  $L_1$ -norm based 2DPCA (2DPCA- $L_1$ ) [24] and 2DPCA- $L_1$  with sparsity (2DPCA- $L_1$ S) [25] are two typical improvements of PCA-

• Z.-G. Jia is with the School of Mathematics and Statistics, Jiangsu Normal University, Xuzhou 221116, China; and with the Research Institute of Mathematical Science, Jiangsu Normal University, Xuzhou 221116, China.

E-mail: zhgjia@jsnu.edu.cn

• Z.-J. Qiu is with the School of Mathematics and Statistics, Jiangsu Normal University, Xuzhou 221116, China.

• M.-X. Zhao is with School of Information and Control Engineering, China University of Mining and Technology, Xuzhou 221116, China; and with the School of Mathematics and Statistics, Jiangsu Normal University, Xuzhou 221116, China.

$L_1$  and RSPCA, respectively. And the generalized 2DPCA (G2DPCA) [26] imposes  $L_p$ -norm on both objective and constraint functions of 2DPCA. Recently, Jia *et al.* [27] further proposed the R2DPCA algorithm, which utilizes the label information (if known) of training samples to calculate a relaxation vector and presents a weight to each subset of training data.

To process color images, the above method separately processes three color channels or connects the representations of different color channels into a large matrix, so cross-channel correlation is not considered [28], [29]. However, this correlation is very important for color image processing. Xiang *et al.* [30] proposed a CPCCA approach for color face recognition. They utilized a color image matrix representation model based on the framework of PCA and applied 2DPCA to compute the optimal projection for feature extraction. Zou *et al.* [31] then presented quaternion collaborative representation-based classification (QCRC) and quaternion sparse RC (QSRC) using quaternion  $L_1$  minimization. For color face recognition, a series of quaternion-based methods, such as the quaternion PCA (QPCA) [32], the two-dimensional QPCA (2DQPCA), the bidirectional 2DQPCA [33], the kernel QPCA (KQPCA) and the two-dimensional KQPCA [34], have been proposed, with generalizing the conventional PCA and 2DPCA. Recently, Jia *et al.* [1] presented the 2DQPCA approach based on quaternion models with reducing the feature dimension in row direction, which is a generalization of the 2DPCA method proposed by Yang *et al.* [6]. Xiao and Zhou [3] proposed novel quaternion ridge regression models for 2DQPCA with reducing the feature dimension in column direction and two-dimensional quaternion sparse principle component analysis. Jia *et al.* [2] further improved the 2DQPCA into abstracting the features of quaternion matrix samples in both row and column directions. Lately, Xiao *et al.* [4] proposed a two-dimensional quaternion sparse discriminant analysis (2D-QSDA), including sparse regularization, that meets the requirements of representing RGB and RGB-D images. These 2DQPCA-like approaches can preserve the spatial structure of color images and have a low computation cost. They have achieved a significant success in promoting the robustness and the ratio of face recognition by utilizing color information.

In addition to PCA-like methods, LDA and its variants are still one kind of feature extraction algorithms which play an important role in pattern recognition and computer vision, see [35]- [37] for instance. Besides of color face recognition, many recent studies (e.g. [38]-[41]) also have shown that quaternion framework are well adapted to color image restoration by encoding the color channels into the three imaginary parts.

The contribution of this paper is listed in three aspects.

- A novel generalized two-dimensional quaternion principal component analysis (G2DQPCA) is presented by generalizing the  $L_2$ -norm of 2DQPCA [1] to the  $L_p$ -norm. G2DQPCA is a general framework that offers the great flexibility to fit various real-world applications, and includes 2DQPCA, sparse 2DQPCA, 2DQPCA- $L_1$ , etc.
- The framework of minorization-maximization (MM) [42] is extended to the quaternion domain to com-

pute the optimal projection bases of G2DQPCA. To utilize the first-order condition of convex quaternion function, a new definition is proposed for the derivative of the quaternion norm. A closed-form solution is obtained at each step of iteration. A strict theoretical analysis is firstly proposed.

- A new weighted G2DQPCA (WG2DQPCA) approach is proposed for color face recognition, as well as a G2DQPCA approach for color image reconstruction. The projection bases are mathematically required to be orthogonal to each other and are weighted by corresponding objective function value to enhance the role of main features in color image recognition. In numerical experiments on practical color face databases, WG2DQPCA and G2DQPCA perform better than the state-of-the-art methods.

The paper is organized as follows. In section 2, we recall the fundamental information of quaternion matrix theory. In section 3, we present a generalized two-dimensional color principal component analysis with weighted projection approach based on quaternion models and give a closed-form solution to this problem. In section 4, we present the WG2DQPCA and G2DQPCA approaches for face recognition and image reconstruction, respectively. In section 5, numerical experiments are conduct by applying the Georgia Tech face database, color FERET face database and the Faces95 database. Finally, the conclusion is given in section 6.

## 2 PRELIMINARIES

In this section, we recall the basic information of quaternions, quaternion vectors and quaternion matrices.

Let us firstly describe some notation. Letters of regular font denote scalars, vectors and matrices in the real domain. Boldface letters denote quaternions, quaternion vectors and quaternion matrices.  $\text{Sign}(\cdot)$  denotes the sign function;  $|\cdot|$  denotes the absolute value;  $w \circ v$  denotes the Hadamard product, i.e., the element-wise product between two vectors;  $\|\cdot\|_1$ ,  $\|\cdot\|_2$ , and  $\|\cdot\|_p$  denote  $L_1$ -norm,  $L_2$ -norm, and  $L_p$ -norm, respectively.

Let  $\mathbf{i}$ ,  $\mathbf{j}$ ,  $\mathbf{k}$  be three imaginary units satisfying

$$\mathbf{i}^2 = \mathbf{j}^2 = \mathbf{k}^2 = \mathbf{ijk} = -1. \quad (2.1)$$

and  $\mathbb{Q} = \left\{ \mathbf{a} = a^{(0)} + a^{(1)}\mathbf{i} + a^{(2)}\mathbf{j} + a^{(3)}\mathbf{k} \mid a^{(0)}, \dots, a^{(3)} \in \mathbb{R} \right\}$  denote the quaternion skew-field.

**DEFINITION 2.1.** For a quaternion number  $\mathbf{a} \in \mathbb{Q}$  and  $s > 0$ , the generalized absolute value is defined by

$$|\mathbf{a}|_s = \sqrt[s]{|a^{(0)}|^s + |a^{(1)}|^s + |a^{(2)}|^s + |a^{(3)}|^s}.$$

$|\mathbf{a}|_s$  is called the  $s$ -absolute value of  $\mathbf{a}$ . If  $s = 2$ , then  $|\mathbf{a}|_s$  is exactly the absolute of  $\mathbf{a}$ , shortly denoted by  $|\mathbf{a}|$ . For illustration, we plot the set of purely quaternion numbers satisfying  $|\mathbf{a}|_s \leq 1$  in Figure 2.1. The sign of the quaternion  $\mathbf{a}$  is defined by

$$\text{sign}(\mathbf{a}) = \begin{cases} \mathbf{a}/|\mathbf{a}|, & \text{if } \mathbf{a} \neq 0, \\ 0, & \text{if } \mathbf{a} = 0. \end{cases} \quad (2.2)$$

An  $m \times n$  quaternion matrix is of the form  $\mathbf{A} = A^{(0)} + A^{(1)}\mathbf{i} + A^{(2)}\mathbf{j} + A^{(3)}\mathbf{k}$ , where  $A^{(0)}, \dots, A^{(3)} \in \mathbb{R}^{m \times n}$ . A

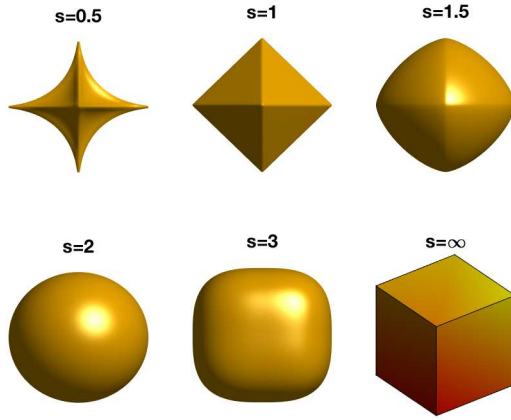


Fig. 2.1: Purely imaginary quaternions with  $s$ -absolute values equal to or less than 1 ( $|\mathbf{a}|_s \leq 1$ ).

quaternion is a *pure quaternion* if its real part is zero. A *pure quaternion matrix* is a matrix whose elements are pure quaternions ( $A^{(0)} = 0$ ) or zero. In the RGB color space, a pixel can be represented with a pure quaternion,  $r\mathbf{i} + g\mathbf{j} + b\mathbf{k}$ , where  $r, g, b$  stand for the values of Red, Green and Blue components, respectively. An  $m \times n$  color image can be saved as an  $m \times n$  pure quaternion matrix,  $\mathbf{A} = [\mathbf{a}_{ij}]_{m \times n}$ , in which each element,  $\mathbf{a}_{ij} = r_{ij}\mathbf{i} + g_{ij}\mathbf{j} + b_{ij}\mathbf{k}$ , denotes one color pixel, and  $r_{ij}, g_{ij}$  and  $b_{ij}$  are nonnegative integers [40], [43].

## 2.1 Norms of quaternion vectors

An  $n$ -dimensional quaternion vector is of the form

$$\mathbf{w} = [\mathbf{w}_i]_n = w^{(0)} + w^{(1)}\mathbf{i} + w^{(2)}\mathbf{j} + w^{(3)}\mathbf{k}, \quad (2.3)$$

where  $\mathbf{w}_i \in \mathbb{Q}$  denotes the  $i$ -th entry of  $\mathbf{w}$ , and  $w^{(0)}, \dots, w^{(3)} \in \mathbb{R}^n$ . The sign and the absolute value of a quaternion vector are defined in the element-wise manner, that is

$$|\mathbf{w}| = [|\mathbf{w}_i|]_n, \quad (2.4a)$$

$$\text{sign}(\mathbf{w}) = [\text{sign}(\mathbf{w}_i)]_n. \quad (2.4b)$$

Clearly, if  $\mathbf{w}$  has no zero entry then

$$\text{sign}(\mathbf{w}) = \left[ \frac{w_i^{(0)}}{|\mathbf{w}_i|} \right]_n + \left[ \frac{w_i^{(1)}}{|\mathbf{w}_i|} \right]_n \mathbf{i} + \left[ \frac{w_i^{(2)}}{|\mathbf{w}_i|} \right]_n \mathbf{j} + \left[ \frac{w_i^{(3)}}{|\mathbf{w}_i|} \right]_n \mathbf{k}.$$

**DEFINITION 2.2.** Let  $s$  and  $p$  be two positive real numbers, the  $L_{s,p}$ -norm of a quaternion vector  $\mathbf{w} \in \mathbb{Q}^n$  is defined by

$$\|\mathbf{w}\|_{s,p} = \left( \sum_{i=1}^n |\mathbf{w}_i|_s^p \right)^{\frac{1}{p}}. \quad (2.5)$$

If  $s = p = 2$ , the  $L_{s,p}$ -norm reduces to the  $L_2$  norm. Because the  $s$ -absolute value quaternions have different geometric properties, people expect to apply different  $L_{s,p}$ -norms in the regularization constrains to obtain especial features of color images. In the following text, we always set  $s$  as the default value 2, and drop  $s$  from the subscript for simplicity. That is the  $L_p$  norm of quaternion vector  $\mathbf{w}$ ,

$$\|\mathbf{w}\|_p = \left( \sum_{i=1}^n |\mathbf{w}_i|^p \right)^{\frac{1}{p}}. \quad (2.6)$$

## 2.2 The real structure-preserving method

Since the computation of quaternion matrices usually costs a lot of CPU times, we always apply the structure-preserving method (see [44], [45], etc.) to simulate the calculation of quaternions only by real operations.

For quaternion matrix  $\mathbf{A} = A^{(0)} + A^{(1)}\mathbf{i} + A^{(2)}\mathbf{j} + A^{(3)}\mathbf{k} \in \mathbb{Q}^{m \times n}$  and quaternion vector  $\mathbf{w} = w^{(0)} + w^{(1)}\mathbf{i} + w^{(2)}\mathbf{j} + w^{(3)}\mathbf{k} \in \mathbb{Q}^n$ , we define their real representations by

$$\mathbf{A}^{(\gamma)} \equiv \begin{bmatrix} A^{(0)} & -A^{(1)} & -A^{(2)} & -A^{(3)} \\ A^{(1)} & A^{(0)} & -A^{(3)} & A^{(2)} \\ A^{(2)} & A^{(3)} & A^{(0)} & -A^{(1)} \\ A^{(3)} & -A^{(2)} & A^{(1)} & A^{(0)} \end{bmatrix} \quad (2.7)$$

and

$$\mathbf{w}^{(\gamma)} \equiv [ (w^{(0)})^T \ (w^{(1)})^T \ (w^{(2)})^T \ (w^{(3)})^T ]^T, \quad (2.8)$$

respectively. The absolute value and sign of  $\mathbf{w}^{(\gamma)}$  are defined by

$$\text{absQ}(\mathbf{w}^{(\gamma)}) = (|\mathbf{w}| + |\mathbf{w}|\mathbf{i} + |\mathbf{w}|\mathbf{j} + |\mathbf{w}|\mathbf{k})^{(\gamma)}, \quad (2.9a)$$

$$\text{signQ}(\mathbf{w}^{(\gamma)}) = (\text{sign}(\mathbf{w}))^{(\gamma)}. \quad (2.9b)$$

The  $L_p$ -norm of quaternion vector  $\mathbf{w}^{(\gamma)}$  is defined by

$$\|\mathbf{w}^{(\gamma)}\|_{2,p} \equiv \left[ \sum_{i=1}^n \left( \sqrt{\sum_{k=0}^3 (\mathbf{w}_{kn+j}^{(\gamma)})^2} \right)^p \right]^{\frac{1}{p}}. \quad (2.10)$$

It's easy to verify that  $\|\mathbf{w}^{(\gamma)}\|_{2,p}$  is a vector norm on the real vector space if  $p \geq 1$ . If  $0 < p < 1$ ,  $\|\mathbf{w}^{(\gamma)}\|_{2,p}$  is regard as a non-convex and non-Lipschitz continuous function. In fact, the  $L_p$ -norm of quaternion vector  $\mathbf{w}$  can be further written as

$$\|\mathbf{w}\|_p^p = \sum_{i=1}^n |\mathbf{w}_i|^p = \sum_{i=1}^n \left( \sqrt{\sum_{j=0}^3 (w_i^{(j)})^2} \right)^p.$$

Hence,

$$\|\mathbf{w}\|_p^p = \|\mathbf{w}^{(\gamma)}\|_{2,p}^p. \quad (2.11)$$

## 3 GENERALIZED 2DQPCA

In this section, we present a new generalized 2DQPCA (G2DQPCA) and quaternion optimization algorithms.

### 3.1 G2DQPCA

Suppose that  $\mathbf{F}_1, \mathbf{F}_2, \dots, \mathbf{F}_\ell \in \mathbb{Q}^{m \times n}$  are  $\ell$  training samples of the quaternion matrix form and their mean is

$$\Psi = \frac{1}{\ell} \sum_{s=1}^{\ell} \mathbf{F}_s \in \mathbb{Q}^{m \times n}. \quad (3.1)$$

Without loss of generality, the training samples are assumed to be centralized, that is,  $\Psi = 0$ . In the new G2DQPCA, the features are extracted by solving a quaternion optimization model:

$$\begin{aligned} (\hat{\mathbf{w}}_1, \dots, \hat{\mathbf{w}}_k) = & \arg \max_{\mathbf{w}_1, \dots, \mathbf{w}_k \in \mathbb{Q}^n} \sum_{j=1}^k \sum_{i=1}^{\ell} \|\mathbf{F}_i \mathbf{w}_j\|_s^s, \\ s.t. \|\mathbf{w}_j\|_p^p = 1, \mathbf{w}_j^* \mathbf{w}_i = 0, i \neq j, i, j = 1, \dots, k, \end{aligned} \quad (3.2)$$

where  $s \geq 1, p > 0$ . Here, the  $L_p$ -norms are applied in both the objective function and the constraint function. The

constraint  $\|\mathbf{w}_j\|_p^p = 1$  is convex if  $p \geq 1$  and non-convex if  $0 < p < 1$ . This makes the constraint set either convex or nonconvex depending on the value of  $p$ .

Now we are concerned with the solvability of the optimization problem with  $L_p$ -norm (3.2). As primary results, several necessary inequalities are derived for a linear optimization problem in quaternion domain with  $L_p$ -norm. Their proofs are based on the first-order condition of convex function [11]. Let  $w, v \in \mathbb{R}^n$  be two real vectors and a real function  $f(w)$  of real vectors be convex and differentiable. Then

$$f(w) \geq f(v) + \nabla f(v)^T(w - v), \quad (3.3)$$

where  $\nabla$  denotes the gradient operator, and the equality holds when  $w = v$ .

**THEOREM 3.1.** *Let  $\mathbf{w}, \mathbf{v} \in \mathbb{Q}^n$  be two quaternion vectors and  $p \geq 1$ , then there is*

$$\begin{aligned} \|\mathbf{w}\|_p^p &\geq p[\text{absQ}(\mathbf{v}^{(\gamma)})^{p-1} \circ \text{signQ}(\mathbf{v}^{(\gamma)})]^T \mathbf{w}^{(\gamma)} \\ &\quad + (1-p)\|\mathbf{v}\|_p^p \end{aligned} \quad (3.4)$$

and the equality holds when  $\mathbf{w} = \mathbf{v}$ .

*Proof.* Denote  $\mathbf{w} = [\mathbf{w}_1, \dots, \mathbf{w}_n]^T$ ,  $\mathbf{v} = [\mathbf{v}_1, \dots, \mathbf{v}_n]^T$ ,  $\mathbf{w}_i, \mathbf{v}_i \in \mathbb{Q}$ . By the real structure-preserving method, we only need to prove

$$\begin{aligned} \|\mathbf{w}^{(\gamma)}\|_{2,p}^p &\geq p[\text{absQ}(\mathbf{v}^{(\gamma)})^{p-1} \circ \text{signQ}(\mathbf{v}^{(\gamma)})]^T \mathbf{w}^{(\gamma)} \\ &\quad + (1-p)\|\mathbf{v}^{(\gamma)}\|_{2,p}^p. \end{aligned} \quad (3.5)$$

Firstly, we assume all entries of  $\mathbf{v}$  are non-zero elements. Then  $\|\mathbf{w}^{(\gamma)}\|_{2,p}^p$  is differentiable at  $\mathbf{w}^{(\gamma)} = \mathbf{v}^{(\gamma)}$ , and

$$\frac{\partial \|\mathbf{w}^{(\gamma)}\|_{2,p}^p}{\partial \mathbf{w}^{(\gamma)}} = \begin{bmatrix} y_0 \\ y_1 \\ y_2 \\ y_3 \end{bmatrix}, \quad (3.6)$$

where

$$y_j = \begin{bmatrix} p \frac{|\mathbf{w}_1|^{p-1}}{|\mathbf{w}_1|} w_1^{(j)} \\ p \frac{|\mathbf{w}_2|^{p-1}}{|\mathbf{w}_2|} w_2^{(j)} \\ \vdots \\ p \frac{|\mathbf{w}_n|^{p-1}}{|\mathbf{w}_n|} w_n^{(j)} \end{bmatrix}, \quad j = 0, 1, 2, 3.$$

Applying the definition (2.9), we obtain

$$\begin{aligned} \nabla \|\mathbf{v}^{(\gamma)}\|_{2,p}^p &\equiv \frac{\partial \|\mathbf{w}^{(\gamma)}\|_{2,p}^p}{\partial \mathbf{w}^{(\gamma)}}|_{\mathbf{w}=\mathbf{v}} \\ &= p \cdot \text{absQ}(\mathbf{v}^{(\gamma)})^{p-1} \circ \text{signQ}(\mathbf{v}^{(\gamma)}). \end{aligned} \quad (3.7)$$

Clearly,

$$\begin{aligned} &(\text{absQ}(\mathbf{v}^{(\gamma)})^{p-1} \circ \text{signQ}(\mathbf{v}^{(\gamma)}))^T \mathbf{v}^{(\gamma)} \\ &= \sum_{j=0}^3 \sum_{i=1}^n \frac{|\mathbf{v}_i|^{p-1}}{|\mathbf{v}_i|} (v_i^{(j)})^2 \\ &= \sum_{i=1}^n \frac{|\mathbf{v}_i|^{p-1}}{|\mathbf{v}_i|} \left( \sum_{j=0}^3 (v_i^{(j)})^2 \right) \\ &= \sum_{i=1}^n \frac{|\mathbf{v}_i|^{p-1}}{|\mathbf{v}_i|} |\mathbf{v}_i|^2 \\ &= \|\mathbf{v}^{(\gamma)}\|_{2,p}^p. \end{aligned} \quad (3.8)$$

Additionally,  $\|\mathbf{w}^{(\gamma)}\|_{2,p}^p$  is a convex function because  $p \geq 1$ . Together with equality (3.7), the first-order convexity condition (3.3), applied to the function  $f(\cdot) = \|\cdot\|_{2,p}^p$ , yields the desired result

$$\begin{aligned} &\|\mathbf{w}^{(\gamma)}\|_{2,p}^p \\ &\geq \|\mathbf{v}^{(\gamma)}\|_{2,p}^p + (\nabla \|\mathbf{v}^{(\gamma)}\|_{2,p}^p)^T (\mathbf{w}^{(\gamma)} - \mathbf{v}^{(\gamma)}) \\ &= p[\text{absQ}(\mathbf{v}^{(\gamma)})^{p-1} \circ \text{signQ}(\mathbf{v}^{(\gamma)})]^T \mathbf{w}^{(\gamma)} \\ &\quad + (1-p)\|\mathbf{v}^{(\gamma)}\|_{2,p}^p \end{aligned} \quad (3.9)$$

where the equality holds when  $\mathbf{w} = \mathbf{v}$ .

Now we consider the case that  $\mathbf{v}$  has zero entries. For any two quaternions  $\mathbf{w}_i$  and  $\mathbf{v}_i$ , there is

$$\begin{aligned} |\mathbf{w}_i|^p &\geq p \cdot |\mathbf{v}_i|^{p-1} \cdot (\text{signQ}(\mathbf{v}_i^{(\gamma)}))^T \mathbf{w}_i^{(\gamma)} \\ &\quad + (1-p)|\mathbf{v}_i|^p. \end{aligned} \quad (3.10)$$

If  $\mathbf{v}_i \neq 0$ , this inequality is exactly (3.9) being applied to two quaternions, because  $|\mathbf{w}_i|^p = \left( \sqrt{\sum_{j=0}^3 (w_i^{(j)})^2} \right)^p$  is convex and differentiable at  $\mathbf{w}_i = \mathbf{v}_i$ . If  $\mathbf{v}_i = 0$ , the inequality (3.10) reduces to  $|\mathbf{w}_i|^p \geq 0$ , and surely holds since  $\text{signQ}(\mathbf{v}_i^{(\gamma)}) = 0$  according the definition (2.9b) (and under the assumption  $0^0 = 1$ ). The equality in (3.10) holds when  $\mathbf{w}_i = \mathbf{v}_i$ . Summing up (3.10) together with  $i = 1, \dots, n$ , we obtain

$$\begin{aligned} &\sum_{i=1}^n \left( \sqrt{\sum_{j=0}^3 (w_i^{(j)})^2} \right)^p \\ &\geq p \sum_{i=1}^n \left[ |\mathbf{v}_i|^{p-1} \cdot (\text{signQ}(\mathbf{v}_i^{(\gamma)}))^T \mathbf{w}_i^{(\gamma)} \right] \\ &\quad + (1-p) \sum_{i=1}^n \left( \sqrt{\sum_{j=0}^3 (v_i^{(j)})^2} \right)^p. \end{aligned} \quad (3.11)$$

Consequently, (3.5) holds and the inequality becomes equality when  $\mathbf{w} = \mathbf{v}$  no matter  $\mathbf{v}$  has zero entries or not. This completes the proof.  $\square$

Let  $w \in \mathbb{R}^n$ ,  $v \in \mathbb{R}^n$ , and  $p, q \in [1, \infty]$  be two scalars with  $1/p + 1/q = 1$ . Then the Hölder's inequality [46] states that

$$\sum_{i=1}^n |v_i w_i| \leq \|v\|_q \|w\|_p. \quad (3.12)$$

The equality holds if and only if there exists a positive real scalar  $c$  satisfying  $|w_i|^p = c|v_i|^q$ ,  $i = 1, 2, \dots, n$ . Since two arbitrary quaternions are not comparable, here we consider the linear optimization problem with  $L_p$ -norm based on the Hölder's inequality.

**LEMMA 3.2.** *Let  $\mathbf{w} \in \mathbb{Q}^n$ ,  $\mathbf{v} \in \mathbb{Q}^n \setminus \{0\}$ , and let  $p, q \in [1, \infty]$  be two scalars satisfying  $1/p + 1/q = 1$ . Then the quaternion optimization problem*

$$\max_{\mathbf{w}} \text{Real}(\mathbf{v}^* \mathbf{w}), \quad \text{s.t. } \|\mathbf{w}\|_p^p = 1 \quad (3.13)$$

has a closed-form solution

$$\mathbf{w}^{(\gamma)} = \frac{(\text{absQ}(\mathbf{v}^{(\gamma)}))^{q-1}}{\|\mathbf{v}^{(\gamma)}\|_{2,q}^{q-1}} \circ \text{signQ}(\mathbf{v}^{(\gamma)}). \quad (3.14)$$

*Proof.* According to the representation (2.8), the quaternion optimization problem (3.13) is equivalently rewritten to

$$\max_{\mathbf{w}^{(\gamma)}} (\mathbf{v}^{(\gamma)})^T \mathbf{w}^{(\gamma)}, \text{ s.t. } \|\mathbf{w}^{(\gamma)}\|_{2,p}^p = 1. \quad (3.15)$$

Based on the Hölder's inequality (3.12), we have

$$\begin{aligned} (\mathbf{v}^{(\gamma)})^T \mathbf{w}^{(\gamma)} &\leq \sum_{i=1}^n \sum_{j=0}^3 |v_i^{(j)} w_i^{(j)}| \leq \sum_{i=1}^n |\mathbf{v}_i| |\mathbf{w}_i| = |\mathbf{v}|^T |\mathbf{w}| \\ &\leq \|\mathbf{v}\|_q \|\mathbf{w}\|_p = \|\mathbf{v}^{(\gamma)}\|_{2,q} \|\mathbf{w}^{(\gamma)}\|_{2,p} = \|\mathbf{v}^{(\gamma)}\|_{2,q}. \end{aligned}$$

Therefore, the maximum of the objective function is obtained when the inequalities become equalities. The equality in  $(\mathbf{v}^{(\gamma)})^T \mathbf{w}^{(\gamma)} \leq \sum_{i=1}^n \sum_{j=0}^3 |v_i^{(j)} w_i^{(j)}|$  holds when

$$\text{sign}(v_i^{(j)}) = \text{sign}(w_i^{(j)}). \quad (3.16)$$

The equality in  $\sum_{i=1}^n \sum_{j=0}^3 |v_i^{(j)} w_i^{(j)}| \leq \sum_{i=1}^n |\mathbf{v}_i| |\mathbf{w}_i|$  holds when

$$|w_i^{(j)}|^2 = c_i |v_i^{(j)}|^2, \quad j = 0, 1, 2, 3. \quad (3.17)$$

If  $\mathbf{v}_i = 0$ , we set  $c_i = 0$  and  $w_i^{(j)} = 0$ . If  $\mathbf{v}_i \neq 0$ , then the constant  $c_i$  is calculated by

$$c_i = \frac{\sum_{j=0}^3 |w_i^{(j)}|^2}{\sum_{j=0}^3 |v_i^{(j)}|^2} = \frac{|\mathbf{w}_i|^2}{|\mathbf{v}_i|^2}. \quad (3.18)$$

Inputting (3.18) into (3.17) yields the expression

$$\begin{aligned} |w_i^{(j)}| &= \left( c_i |v_i^{(j)}|^2 \right)^{\frac{1}{2}} = \left( \frac{|\mathbf{w}_i|^2}{|\mathbf{v}_i|^2} |v_i^{(j)}|^2 \right)^{\frac{1}{2}} \\ &= \frac{|\mathbf{w}_i|}{|\mathbf{v}_i|} |v_i^{(j)}|. \end{aligned} \quad (3.19)$$

Then we have

$$\begin{aligned} w_i^{(j)} &= \frac{|\mathbf{w}_i|}{|\mathbf{v}_i|} |v_i^{(j)}| \text{sign}(v_i^{(j)}), & \text{if } \mathbf{v}_i \neq 0; \\ w_i^{(j)} &= 0, & \text{if } \mathbf{v}_i = 0. \end{aligned} \quad (3.20)$$

For simplicity, we introduce an auxiliary variable  $Y_i^w$  to denote the absolute of quaternion vector  $\mathbf{w}$ . The equality in  $|\mathbf{v}|^T |\mathbf{w}| \leq \|\mathbf{v}\|_q \|\mathbf{w}\|_p$  holds when

$$|Y_i^w|^p = c |Y_i^v|^q, \quad i = 1, 2, \dots, n. \quad (3.21)$$

Since  $\mathbf{v} \neq 0$ , the constant  $c$  is then calculated by

$$c = \frac{\sum_{i=1}^n |Y_i^w|^p}{\sum_{i=1}^n |Y_i^v|^q} = \frac{\|Y^w\|_p^p}{\|Y^v\|_q^q} = \frac{\|\mathbf{w}^{(\gamma)}\|_{2,p}^p}{\|\mathbf{v}^{(\gamma)}\|_{2,q}^q} = \frac{1}{\|\mathbf{v}^{(\gamma)}\|_{2,q}^q}. \quad (3.22)$$

Substituting (3.22) into (3.21), we have

$$\begin{aligned} |Y_i^w| &= (c |Y_i^v|^q)^{1/p} = \left( \frac{|Y_i^v|^q}{\|Y^v\|_q^q} \right)^{1/p} \\ &= \frac{|Y_i^v|^{q-1}}{\|Y^v\|_q^{q-1}}, \quad i = 1, 2, \dots, n, \end{aligned} \quad (3.23)$$

i.e.

$$\|\mathbf{w}_i\|_2 = \frac{\|\mathbf{v}_i\|_2^{q-1}}{\|\mathbf{v}^{(\gamma)}\|_{2,q}^{q-1}}. \quad (3.24)$$

Together with equality (3.20), we obtain the expression

$$\begin{aligned} w_i^{(j)} &= \frac{\|\mathbf{v}_i\|_2^{q-1}}{\|\mathbf{v}^{(\gamma)}\|_{2,q}^{q-1}} \frac{1}{\|\mathbf{v}_i\|_2} |v_i^{(j)}| \text{sign}(v_i^{(j)}) \\ &= \frac{|\mathbf{v}_i|^{q-1}}{\|\mathbf{v}^{(\gamma)}\|_{2,q}^{q-1}} \frac{v_i^{(j)}}{|\mathbf{v}_i|}. \end{aligned} \quad (3.25)$$

Connecting to the definition (2.9) and rewriting the equation into vector form, we yields the desired result

$$\mathbf{w}^{(\gamma)} = \frac{(\text{absQ}(\mathbf{v}^{(\gamma)}))^{q-1}}{\|\mathbf{v}^{(\gamma)}\|_{2,q}^{q-1}} \circ \text{signQ}(\mathbf{v}^{(\gamma)}). \quad (3.26)$$

The proof is completed.  $\square$

**LEMMA 3.3.** Let  $\mathbf{w} = [\mathbf{w}_i]$ ,  $\mathbf{v} = [\mathbf{v}_i] \in \mathbb{Q}^n$  with  $\mathbf{w}_i \neq 0$  and  $\mathbf{v}_i \neq 0$  for any  $1 \leq i \leq n$ , and  $0 < p < 1$ . Then

$$\|\mathbf{w}\|_p^p \leq p(|\mathbf{v}|^{p-1})^T |\mathbf{w}| + (1-p) \|\mathbf{v}\|_p^p \quad (3.27)$$

holds wherein the inequality becomes equality when  $|\mathbf{w}| = |\mathbf{v}|$ .

*Proof.* Recall that the absolute value function is defined in (2.4a). For any quaternion vector  $\mathbf{w}$  with each entry  $\mathbf{w}_i \neq 0$ ,  $|\mathbf{w}|$  is a real vector with positive entries. Let  $f(|\mathbf{w}|) = \|\mathbf{w}\|_p$ , then  $f(\cdot)$  is convex and differentiable at positive real vector when  $0 < p < 1$ . From the first-order convexity condition (3.3), we obtain  $\|\mathbf{w}\|_p^p \leq p(|\mathbf{v}|^{p-1} \circ \text{sign}(|\mathbf{v}|))^T |\mathbf{w}| + (1-p) \|\mathbf{v}\|_p^p$ . Apparently, if  $\mathbf{w}^{(\gamma)} = \mathbf{v}^{(\gamma)}$ , it must satisfy the condition that  $|\mathbf{w}| = |\mathbf{v}|$ .  $\square$

Note that in our method, in order to meet the condition that  $\mathbf{w}_i \neq 0$  and  $\mathbf{v}_i \neq 0$ , if any element in the projection vector  $(\mathbf{w}^{(\gamma)})^{(k)}$  is zero, then we replace it with  $(\mathbf{w}^{(\gamma)})^{(k)} + \varepsilon$  to make sure that it has no zero elements, where  $\varepsilon$  is a random scalar that is sufficiently close to zero.

### 3.1.1 Case 1: Convex constraint set

Now, we proceeding to the solution of G2DQPCA problem for the first case, i.e.,  $p \geq 1$ , based on Theorem 3.1 and Lemma 3.2.

The quaternion optimization problem of G2DQPCA states

$$\max_{\mathbf{w}} \sum_{i=1}^{\ell} \|\mathbf{F}_i \mathbf{w}\|_s^s, \text{ s.t. } \|\mathbf{w}\|_p^p = 1, \quad (3.28)$$

where  $s \geq 1, p \geq 1, \mathbf{w} \in \mathbb{Q}^n$ . The constraint set is convex. According to equality (2.7) and (2.8), the quaternion optimization problem (3.28) can be transformed to its equivalent real counterpart,

$$\max_{\mathbf{w}^{(\gamma)}} \sum_{i=1}^{\ell} \|\mathbf{F}_i^{(\gamma)} \mathbf{w}^{(\gamma)}\|_{2,s}^s, \text{ s.t. } \|\mathbf{w}^{(\gamma)}\|_p^p = 1. \quad (3.29)$$

This real optimization problem can be turned into iteratively maximizing a surrogate function under the MM framework, as shown below. Assume  $(\mathbf{w}^{(\gamma)})^{(k)}$  is the projection vector at the  $k$ -th step in the iteration procedure. It could be regarded as a constant vector that is irrelevant with respect to  $\mathbf{w}^{(\gamma)}$ . Define

$$\hat{F}_i = \text{absQ}(\mathbf{F}_i^{(\gamma)} (\mathbf{w}^{(\gamma)})^{(k)})^{s-1} \circ \text{signQ}(\mathbf{F}_i^{(\gamma)} (\mathbf{w}^{(\gamma)})^{(k)}),$$

according to Theorem 3.1. The convex objective function could be linearized as

$$\begin{aligned} \sum_{i=1}^{\ell} \|\mathbf{F}_i \mathbf{w}\|_s^s &= \sum_{i=1}^{\ell} \|\mathbf{F}_i^{(\gamma)} \mathbf{w}^{(\gamma)}\|_{2,s}^s \\ &\geq s \sum_{i=1}^{\ell} \hat{F}_i^T \mathbf{F}_i^{(\gamma)} \mathbf{w}^{(\gamma)} + (1-s) \sum_{i=1}^{\ell} \|\mathbf{F}_i^{(\gamma)} (\mathbf{w}^{(\gamma)})^{(k)}\|_{2,s}^s, \end{aligned} \quad (3.30)$$

wherein the inequality becomes equality when  $\mathbf{w}^{(\gamma)} = (\mathbf{w}^{(\gamma)})^{(k)}$ . Denote the objective function by  $f(\mathbf{w}^{(\gamma)})$ , and the linearized function by  $g(\mathbf{w}^{(\gamma)} | (\mathbf{w}^{(\gamma)})^{(k)})$ . That is

$$f(\mathbf{w}^{(\gamma)}) = \sum_{i=1}^{\ell} \|\mathbf{F}_i^{(\gamma)} \mathbf{w}^{(\gamma)}\|_{2,s}^s, \quad (3.31)$$

and

$$\begin{aligned} g(\mathbf{w}^{(\gamma)} | (\mathbf{w}^{(\gamma)})^{(k)}) &= s \sum_{i=1}^{\ell} \hat{F}_i^T \mathbf{F}_i^{(\gamma)} \mathbf{w}^{(\gamma)} \\ &\quad + (1-s) \sum_{i=1}^{\ell} \|\mathbf{F}_i^{(\gamma)} (\mathbf{w}^{(\gamma)})^{(k)}\|_{2,s}^s. \end{aligned} \quad (3.32)$$

According to (3.8) and by simple algebra, it is easy to verify that

$$\hat{F}_i^T \mathbf{F}_i^{(\gamma)} (\mathbf{w}^{(\gamma)})^{(k)} = \|\mathbf{F}_i^{(\gamma)} (\mathbf{w}^{(\gamma)})^{(k)}\|_{2,s}^s.$$

Then we have  $f((\mathbf{w}^{(\gamma)})^{(k)}) = g((\mathbf{w}^{(\gamma)})^{(k)} | (\mathbf{w}^{(\gamma)})^{(k)})$  and  $f(\mathbf{w}^{(\gamma)}) \geq g(\mathbf{w}^{(\gamma)} | (\mathbf{w}^{(\gamma)})^{(k)})$  for all  $\mathbf{w}^{(\gamma)}$ , satisfying the two key conditions of the MM framework [42]. Therefore,  $g(\mathbf{w}^{(\gamma)} | (\mathbf{w}^{(\gamma)})^{(k)})$  is a feasible surrogate function of  $f(\mathbf{w}^{(\gamma)})$ . According to the MM framework, the optimization problem in (3.28) could be turned into iteratively maximizing the surrogate function as follows

$$\begin{aligned} (\mathbf{w}^{(\gamma)})^{k+1} &= \arg \max_{\mathbf{w}^{(\gamma)}} g(\mathbf{w}^{(\gamma)} | (\mathbf{w}^{(\gamma)})^{(k)}), \\ \text{s.t. } \|\mathbf{w}^{(\gamma)}\|_{2,p}^p &= 1. \end{aligned} \quad (3.33)$$

Define

$$(\mathbf{v}^{(\gamma)})^{(k)} = \sum_{i=1}^{\ell} (\mathbf{F}_i^{(\gamma)})^T \hat{F}_i, \quad (3.34)$$

by dropping the term irrelevant to  $\mathbf{w}^{(\gamma)}$  in the surrogate function (3.32), maximizing the surrogate function leads to a linear optimization problem with  $L_p$ -norm constraint

$$\begin{aligned} (\mathbf{w}^{(\gamma)})^{(k+1)} &= \arg \max_{\mathbf{w}^{(\gamma)}} g(\mathbf{w}^{(\gamma)} | (\mathbf{w}^{(\gamma)})^{(k)}) \\ &= \arg \max_{\mathbf{w}^{(\gamma)}} [(\mathbf{v}^{(\gamma)})^{(k)}]^T \mathbf{w}^{(\gamma)}, \\ \text{s.t. } \|\mathbf{w}^{(\gamma)}\|_{2,p}^p &= 1. \end{aligned} \quad (3.35)$$

According to Lemma 3.2, the solution of this problem is

$$(\mathbf{w}^{(\gamma)})^{(k+1)} = \frac{\text{absQ}((\mathbf{v}^{(\gamma)})^{(k)})^{q-1}}{\|(\mathbf{v}^{(\gamma)})^{(k)}\|_{2,q}^{q-1}} \circ \text{signQ}((\mathbf{v}^{(\gamma)})^{(k)}), \quad (3.36)$$

where  $q$  satisfies  $\frac{1}{p} + \frac{1}{q} = 1$ . The solution is rewritten in a two-step procedure as

$$\begin{aligned} (\mathbf{u}^{(\gamma)})^{(k)} &= \text{absQ}((\mathbf{v}^{(\gamma)})^{(k)})^{q-1} \circ \text{signQ}((\mathbf{v}^{(\gamma)})^{(k)}), \\ (\mathbf{w}^{(\gamma)})^{(k+1)} &= \frac{(\mathbf{u}^{(\gamma)})^{(k)}}{\|(\mathbf{u}^{(\gamma)})^{(k)}\|_{2,p}}. \end{aligned} \quad (3.37)$$

Two extreme condition of case 1, i.e.,  $p = 1$  and  $p = \infty$  are discussed as follows. When  $p = 1$ , we will have  $q = \infty$  according to the relation  $1/p + 1/q = 1$ . Then the denominator of (3.36) becomes  $\|(\mathbf{v}^{(\gamma)})^{(k)}\|_{2,\infty}$ . Let  $j = \arg \max_{i=1, \dots, n} |\mathbf{v}_i^{(k)}|$ , i.e.,  $|\mathbf{v}_j^{(k)}|$  is the largest value in  $|\mathbf{v}^{(k)}|$ . By taking the limit of (3.36) we have

$$\mathbf{w}_i^{(k+1)} = \begin{cases} \text{sign}(\mathbf{v}_i^{(k)}), & i = j, \\ 0, & i \neq j, \end{cases} \quad (3.38)$$

for  $i = 1, 2, \dots, n$ . Similarly, when  $p$  approaches infinity, the limit of (3.36) is

$$(\mathbf{w}^r)^{(k+1)} = \text{signQ}((\mathbf{v}^{(\gamma)})^{(k)}). \quad (3.39)$$

### 3.1.2 Case 2: Nonconvex constraint set

When  $0 < p < 1$ , the constraint set becomes nonconvex. With introducing an auxiliary variable  $Y_i^{\mathbf{w}} \equiv |\mathbf{w}|$ , the the  $L_p$ -norm

$$\|\mathbf{w}\|_p^p = \|Y^{\mathbf{w}}\|_p^p, \quad (3.40)$$

and clearly  $Y^{\mathbf{w}} \in \mathbb{R}^n, Y^{\mathbf{w}} \geq 0$ .

Here we try to apply the method of Lagrange multipliers, considering that the constraint set is non-convex and non-Lipschitz continuous. Maximizing the optimization problem of function (3.2) equals to maximizing the Lagrangian as follows

$$\max_{\mathbf{w}} \sum_{i=1}^{\ell} \|\mathbf{F}_i \mathbf{w}\|_s^s - \lambda (\|\mathbf{w}\|_p^p - 1), \quad (3.41)$$

where  $s \geq 1, 0 < p < 1, \lambda > 0, \mathbf{w} \in \mathbb{Q}^n$ .

Same as in Case 1, we firstly translate this function according to (3.29) and (3.40) into

$$\max_{\mathbf{w}^{(\gamma)}} \sum_{i=1}^{\ell} \|\mathbf{F}_i^{(\gamma)} \mathbf{w}^{(\gamma)}\|_{2,s}^s - \lambda (\|Y^{\mathbf{w}}\|_p^p - 1), \quad (3.42)$$

where  $\|Y^{\mathbf{w}}\|_p^p = \|\mathbf{w}^{(\gamma)}\|_{2,p}^p$  is essentially a function related to  $\mathbf{w}^{(\gamma)}$ . Again, the problem is transformed into iteratively maximizing a surrogate function under the MM framework. Assume that  $(\mathbf{w}^{(\gamma)})^{(k)}$  is the projection vector at the  $k$ -th step in the iteration procedure. If any element in  $(\mathbf{w}^{(\gamma)})^{(k)}$  is zero, then we replace it with  $(\mathbf{w}^{(\gamma)})^{(k)} + \varepsilon$  to make sure that it has no zero elements, where  $\varepsilon$  is a random scalar that is sufficiently close to zero. According to Theorem 3.1 and Lemma 3.3, we have

$$\begin{aligned} &\sum_{i=1}^{\ell} \|\mathbf{F}_i^{(\gamma)} \mathbf{w}^{(\gamma)}\|_{2,s}^s - \lambda (\|Y^{\mathbf{w}}\|_p^p - 1) \\ &\geq s ((\mathbf{v}^{(\gamma)})^{(k)})^T \mathbf{w}^{(\gamma)} + (1-s) \sum_{i=1}^{\ell} \|\mathbf{F}_i^{(\gamma)} (\mathbf{w}^{(\gamma)})^{(k)}\|_{2,s}^s \\ &\quad - \lambda p (|\mathbf{w}^{(k)}|^{p-1} \circ \text{sign}(|\mathbf{w}^{(k)}|))^T Y^{\mathbf{w}} - \lambda (1-p) \|\mathbf{w}^{(k)}\|_p^p \\ &\quad + \lambda, \end{aligned} \quad (3.43)$$

where  $(\mathbf{v}^{(\gamma)})^{(k)}$  is defined in (3.34),

$$|\mathbf{w}^{(k)}| = \begin{bmatrix} |\mathbf{w}_1^{(k)}| & |\mathbf{w}_2^{(k)}| & \dots & |\mathbf{w}_n^{(k)}| \end{bmatrix}^T$$

and this inequality becomes equality when  $\mathbf{w}^{(\gamma)} = (\mathbf{w}^{(\gamma)})^{(k)}$ . Denote the left-hand side of the inequality

by  $f(\mathbf{w}^{(\gamma)})$  and the right-hand side of the inequality by  $g(\mathbf{w}^{(\gamma)}|(\mathbf{w}^{(\gamma)})^{(k)})$ , i.e.,

$$f(\mathbf{w}^{(\gamma)}) = \sum_{i=1}^{\ell} \|\mathbf{F}_i^{(\gamma)} \mathbf{w}^{(\gamma)}\|_{2,s}^s - \lambda(\|Y^{\mathbf{w}}\|_p^p - 1), \quad (3.44)$$

and

$$\begin{aligned} g(\mathbf{w}^{(\gamma)}|(\mathbf{w}^{(\gamma)})^{(k)}) &= s((\mathbf{v}^{(\gamma)})^{(k)})^T \mathbf{w}^{(\gamma)} \\ &+ (1-s) \sum_{i=1}^{\ell} \|\mathbf{F}_i^{(\gamma)} (\mathbf{w}^{(\gamma)})^{(k)}\|_{2,s}^s \\ &- \lambda p(|\mathbf{w}^{(k)}|^{p-1} \circ \text{sign}(|\mathbf{w}^{(k)}|))^T Y^{\mathbf{w}} \\ &- \lambda(1-p)\|\mathbf{w}^{(k)}\|_p^p + \lambda. \end{aligned} \quad (3.45)$$

By the simple algebraic calculation, we obtain

$$f((\mathbf{w}^{(\gamma)})^{(k)}) = g((\mathbf{w}^{(\gamma)})^{(k)}|(\mathbf{w}^{(\gamma)})^{(k)})$$

and

$$f(\mathbf{w}^{(\gamma)}) \geq g(\mathbf{w}^{(\gamma)}|(\mathbf{w}^{(\gamma)})^{(k)})$$

for all  $\mathbf{w}^{(\gamma)}$ , which satisfy the two key conditions of the MM framework. Therefore,  $g(\mathbf{w}^{(\gamma)}|(\mathbf{w}^{(\gamma)})^{(k)})$  is a feasible surrogate function of  $f(\mathbf{w}^{(\gamma)})$ . According to the MM framework, the optimization problem in (3.41) could be turned into iteratively maximizing the surrogate function as follows

$$(\mathbf{w}^{(\gamma)})^{(k+1)} = \arg \max_{\mathbf{w}^{(\gamma)}} g(\mathbf{w}^{(\gamma)}|(\mathbf{w}^{(\gamma)})^{(k)}). \quad (3.46)$$

Then the following quadratic optimization problem will be reached after ignoring irrelevant terms of  $\mathbf{w}^{(\gamma)}$

$$\begin{aligned} (\mathbf{w}^{(\gamma)})^{(k+1)} &= \arg \max_{\mathbf{w}^{(\gamma)}} s((\mathbf{v}^{(\gamma)})^{(k)})^T \mathbf{w}^{(\gamma)} \\ &- \lambda p(|\mathbf{w}^{(k)}|^{p-1} \circ \text{sign}(|\mathbf{w}^{(k)}|))^T Y^{\mathbf{w}}. \end{aligned} \quad (3.47)$$

Let

$$h(\mathbf{w}^{(\gamma)}) = s((\mathbf{v}^{(\gamma)})^{(k)})^T \mathbf{w}^{(\gamma)} - \lambda p(\hat{\mathbf{w}}^{(k)})^T Y^{\mathbf{w}}, \quad (3.48)$$

where  $\hat{\mathbf{w}}^{(k)} = |\mathbf{w}^{(k)}|^{p-1} \circ \text{sign}(|\mathbf{w}^{(k)}|)$  and  $Y^{\mathbf{w}}$  is defined in (3.40). Now we consider the partial derivative with respect to  $\mathbf{w}^{(\gamma)}$

$$\begin{aligned} \left[ \frac{\partial h(\mathbf{w}^{(\gamma)})}{\partial \mathbf{w}^{(\gamma)}} \right]_l &= \frac{\partial h(\mathbf{w}^{(\gamma)})}{\partial w_i^{(j)}} \\ &= s(\mathbf{v}^{(k)})_i^{(j)} - \lambda p \left[ |\mathbf{w}_i^{(k)}|^{p-1} \frac{w_i^{(j)}}{|\mathbf{w}_i|} \right], \end{aligned} \quad (3.49)$$

where  $i = 1, 2, \dots, n, j = 0, 1, 2, 3$  and  $l = 1, 2, \dots, 4n$ .

Let the above equation equal to zero and we get

$$w_i^{(j)} = \frac{s}{\lambda p} (\mathbf{v}^{(k)})_i^{(j)} |\mathbf{w}_i| |\mathbf{w}_i^{(k)}|^{1-p}. \quad (3.50)$$

Rewrite the component as vector expression which is the solution of the problem (3.47)

$$(\mathbf{w}^{(\gamma)})^{(k+1)} = \frac{s}{\lambda p} (\mathbf{v}^{(\gamma)})^{(k)} \circ \tilde{\mathbf{w}}^{(\gamma)}, \quad (3.51)$$

where  $\tilde{\mathbf{w}}^{(\gamma)} = \text{absQ}(\mathbf{w}^{(\gamma)}) \circ \text{absQ}((\mathbf{w}^{(\gamma)})^{(k)})^{1-p}$ . Considering the constraint  $\|\mathbf{w}\|_p^p = 1$ , i.e.  $\|\mathbf{w}^{(\gamma)}\|_{2,p}^p = 1$  and  $\lambda > 0$ , we have

$$\lambda = \frac{s}{p} \|(\mathbf{v}^{(\gamma)})^{(k)} \circ \tilde{\mathbf{w}}^{(\gamma)}\|_{2,p}. \quad (3.52)$$

Then the update rule is

$$(\mathbf{w}^{(\gamma)})^{(k+1)} = \frac{(\mathbf{v}^{(\gamma)})^{(k)} \circ \tilde{\mathbf{w}}^{(\gamma)}}{\|(\mathbf{v}^{(\gamma)})^{(k)} \circ \tilde{\mathbf{w}}^{(\gamma)}\|_{2,p}}. \quad (3.53)$$

The above solution equals to the two-step procedure as below

$$(\mathbf{u}^{(\gamma)})^{(k)} = (\mathbf{v}^{(\gamma)})^{(k)} \circ \tilde{\mathbf{w}}^{(\gamma)}, \quad (3.54)$$

$$(\mathbf{w}^{(\gamma)})^{(k+1)} = \frac{(\mathbf{u}^{(\gamma)})^{(k)}}{\|(\mathbf{u}^{(\gamma)})^{(k)}\|_{2,p}}. \quad (3.55)$$

This completes the solution in Case 2.

Now we have obtained the solution of the quaternion optimization problem of G2DQPCA. From the results in (3.36) and (3.53), we observe that a closed-form solution is obtained in each iteration for both cases.

**REMARK 3.1.** G2DQPCA is a generalization of 2DQPCA with applying  $L_p$ -norm both in the objective function and the constraint function. Let  $s = p = 2$  then G2DQPCA reduces to 2DQPCA [1], [2],

$$\begin{aligned} &\arg \max_{\mathbf{w}_1, \dots, \mathbf{w}_r \in \mathbb{Q}^n} \sum_{j=1}^r \sum_{i=1}^{\ell} \|\mathbf{F}_i \mathbf{w}_j\|_2^2, \\ &\text{s.t. } \begin{cases} \mathbf{w}_j^* \mathbf{w}_i = \|\mathbf{w}_j\|_2^2 = 1 & (i=j), \\ \mathbf{w}_j^* \mathbf{w}_i = 0 & (i \neq j). \end{cases} \end{aligned} \quad (3.56)$$

Indeed, let  $\mathbf{W} = [\mathbf{w}_1, \dots, \mathbf{w}_r]$  then

$$\begin{aligned} &\arg \max_{\mathbf{w}_1, \dots, \mathbf{w}_r \in \mathbb{Q}^n} \sum_{j=1}^r \sum_{i=1}^{\ell} \|\mathbf{F}_i \mathbf{w}_j\|_2^2 = \arg \max_{\mathbf{W} \in \mathbb{Q}^{n \times k}} \sum_{i=1}^{\ell} \|\mathbf{F}_i \mathbf{W}\|_F^2 \\ &= \arg \min_{\mathbf{W} \in \mathbb{Q}^{n \times k}} \sum_{i=1}^{\ell} \|\mathbf{F}_i (\mathbf{I} - \mathbf{W} \mathbf{W}^*)\|_F^2. \end{aligned}$$

The ridge regression model [3] of 2DQPCA is equivalent to the quaternion optimization model (3.56). Notice that the Frobenius norm of a quaternion matrix  $\mathbf{A}$  is defined by  $\|\mathbf{A}\|_F^2 = \text{trace}(\mathbf{A}^* \mathbf{A}) = \text{trace}(\mathbf{A} \mathbf{A}^*)$ .

**REMARK 3.2.** G2DQPCA generalizes G2DPCA from the real field to the quaternion skew-field. Compared with G2DPCA, we firstly constrain the orthogonality of the projection vectors,  $\mathbf{w}_i, i = 1, 2, \dots, r$ , in the ridge regression model (3.2). We will elaborate this constraint later.

### 3.2 A new quaternion optimization algorithm with deflation

Now assume we have obtained the first  $r$  projection vectors, i.e.,  $\mathbf{W} = [\mathbf{w}_1, \mathbf{w}_2, \dots, \mathbf{w}_r]$ , where  $1 \leq r < n$ . The  $(r+1)$ -th projection vector  $\mathbf{w}_{r+1}$  could be calculated similarly on the deflated samples

$$\mathbf{F}_i^{\text{deflated}} = \mathbf{F}_i(\mathbf{I} - \mathbf{W} \mathbf{W}^*), i = 1, 2, \dots, \ell. \quad (3.57)$$

What is particularly noteworthy is that the projection vector  $\mathbf{w}_{r+1}$  obtained at each iteration must be orthonormalized against all previous  $\mathbf{w}_i, i = 1, 2, \dots, r$  by a standard Gram-Schmidt procedure in quaternion domain. This is because when we completed deflation in the  $r$ -th direction that means there is no information left in this direction and then projection on the deflated samples should be zero. We

observe that after  $r$  steps each sample is transformed into (3.57). After deflating samples by  $r$  directions, we obtain that

$$\mathbf{F}_i^{\text{deflated}} \mathbf{w}_j = \mathbf{F}_i(\mathbf{I} - \mathbf{W}\mathbf{W}^*)\mathbf{w}_j = \mathbf{F}_i(\mathbf{w}_j - \mathbf{W} \begin{bmatrix} \mathbf{w}_1^* \\ \mathbf{w}_2^* \\ \vdots \\ \mathbf{w}_r^* \end{bmatrix} \mathbf{w}_j), \quad (3.58)$$

where  $j = 1, 2, \dots, r+1$ .  $\mathbf{F}_i^{\text{deflated}} \mathbf{w}_j$  should be zero if  $j = 1, 2, \dots, r$ . Otherwise the feature information can be lost because of the interference from other direction. From (3.58) with  $j = r+1$ , we also know that the  $(r+1)$ -th projector must not be linearly represented by the prior projectors, or in other words, the newly computed projector is not in the subspace generated by the known projectors, so that we orthogonalize the computed projector to the known ones.

Another notable feature here is the usage of deflation in general. It should not be used to compute more than a few protection vectors because of the fact that the simple matrix  $\mathbf{F}_i$  will accumulate errors from all previous computations and this could be disastrous if the cases where cancellations are so severe in the orthogonalization steps. In our experiments, we use quaternion QR algorithm [45] to complete such orthogonalizing process.

We summarize the above steps into Algorithm 1. Here the notation  $\odot$  is defined by multiplying the corresponding real coefficients between two quaternions. For example, assume  $\mathbf{w} = w_0 + w_1\mathbf{i} + w_2\mathbf{j} + w_3\mathbf{k}$ ,  $\mathbf{v} = v_0 + v_1\mathbf{i} + v_2\mathbf{j} + v_3\mathbf{k}$ , then

$$\mathbf{w} \odot \mathbf{v} = (w_0 \circ v_0) + (w_1 \circ v_1)\mathbf{i} + (w_2 \circ v_2)\mathbf{j} + (w_3 \circ v_3)\mathbf{k}. \quad (3.59)$$

## 4 COLOR IMAGE ANALYSIS WITH WEIGHTED PROJECTION

In this section, we present the weighted G2DQPCA algorithm for color image recognition and the G2DQPCA algorithm for color image reconstruction.

From each iterative step of Algorithm 1, we obtain a maximized value of the objective function corresponding to  $\mathbf{w}_j$ , i.e.,

$$f^{(j)} = \sum_{i=1}^n \|\mathbf{F}_i \mathbf{w}_j^{(k+1)}\|_s^s.$$

Once the algorithm of G2DQPCA is done, we obtain  $r$  pairs of optimal value, denoted by  $(f^{(1)}, \mathbf{w}_1), \dots, (f^{(r)}, \mathbf{w}_r)$ . The contributions of  $\mathbf{w}_1, \dots, \mathbf{w}_r$  to accuracy rate can be characterized by  $f^{(1)}, \dots, f^{(r)}$ . So we weighted each projection  $\mathbf{w}_i$  by multiplying  $f^{(i)}$ ,  $i = 1, \dots, r$ , where  $f^{(i)}$  has been normalized appropriately here. In our experiment in section 5, we normalize the weight coefficient  $f$  by  $f^{(i)}/\sum(f^{(i)})$ . To sum up, the weighted projection are  $\mathbf{w}_1 f^{(1)}, \dots, \mathbf{w}_r f^{(r)}$ . Also, it is obviously to find out that when  $s = p = 2$ , the value of  $f^{(i)}$  is equal to  $i$ th eigenvalue of the covariance matrix of training set.

The eigenface subspace of G2DQPCA is defined by  $\mathbf{W} = [\mathbf{w}_1, \dots, \mathbf{w}_r]$ , in which each  $\mathbf{w}_i$  is computed by Algorithm 1. And the eigenface subspace of WG2DQPCA is defined by  $\mathbf{W} = [\mathbf{w}_1, \dots, \mathbf{w}_r]F$  where  $F = \text{diag}(f^{(i)})$ ,  $i = 1, 2, \dots, r$ .

---

**Algorithm 1** G2DQPCA: the generalized two-dimensional quaternion principal component analysis

---

**Require:** Training samples  $\mathbf{F}_1, \mathbf{F}_2, \dots, \mathbf{F}_\ell$ , the number of selected feature  $r$ , and parameters  $s \in [1, \infty), p \in (0, \infty]$ .  
**Ensure:** Optimal quaternion projection matrix  $\mathbf{W}$ , and weighted coefficient matrix  $\mathbf{D}$

- 1: Initialize  $\mathbf{W} = [\ ]$ ,  $\mathbf{D} = [\ ]$ ,  $\mathbf{F}_i^0 = \mathbf{F}_i$ .
- 2: **for**  $t = 1, 2, \dots, r$  **do**
- 3:   Initialize  $k = 0, \delta = 1$ , arbitrary  $\mathbf{w}^{(0)}$  with  $\|\mathbf{w}^{(0)}\|_p = 1$ .
- 4:    $f^{(0)} = \sum_{i=1}^{\ell} \|\mathbf{F}_i \mathbf{w}^{(0)}\|_s^s$ .
- 5:   **while**  $\delta > 10^{-4}$  **do**
- 6:      $\mathbf{v}^{(k)} = \sum_{i=1}^{\ell} \mathbf{F}_i^* [|\mathbf{F}_i \mathbf{w}^{(k)}|^{s-1} \odot \text{sign}(\mathbf{F}_i \mathbf{w}^{(k)})]$ .
- 7:     **if**  $0 < p < 1$  **then**
- 8:        $\mathbf{u}^{(k)} = |\mathbf{w}^{(0)}| \odot |\mathbf{w}^{(k)}|^{1-p} \odot \mathbf{v}^{(k)}$ ,
- 9:        $\mathbf{w}^{(k+1)} = \frac{\mathbf{u}^{(k)}}{\|\mathbf{u}^{(k)}\|_p}$ .
- 10:     **else if**  $p = 1$  **then**
- 11:        $j = \arg \max_{i \in [1, n]} |\mathbf{v}_i^{(k)}|$ ,
- 12:        $\mathbf{w}_i^{(k+1)} = \begin{cases} \text{sign}(\mathbf{v}_j^{(k)}), & i = j, \\ 0, & i \neq j. \end{cases}$
- 13:     **else if**  $1 < p < \infty$  **then**
- 14:        $q = p/(p-1)$ ,
- 15:        $\mathbf{u}^{(k)} = |\mathbf{v}^{(k)}|^{q-1} \odot \text{sign}(\mathbf{v}^{(k)})$ ,
- 16:        $\mathbf{w}^{(k+1)} = \frac{\mathbf{u}^{(k)}}{\|\mathbf{u}^{(k)}\|_p}$ .
- 17:     **else if**  $p = \infty$  **then**
- 18:        $\mathbf{w}^{(k+1)} = \text{sign}(\mathbf{v}^{(k)})$ .
- 19:     **end if**
- 20:      $f^{(k+1)} = \sum_{i=1}^{\ell} \|\mathbf{F}_i \mathbf{w}^{(k+1)}\|_s^s$ .
- 21:      $\delta = |f^{(k+1)} - f^{(k)}| / |f^{(k)}|$ .
- 22:      $k \leftarrow k + 1$ .
- 23:   **end while**
- 24:    $\mathbf{w}_t = \mathbf{w}^{(k)}$ .
- 25:   Orthogonalize  $\mathbf{w}_t$  with the previous vector  $\mathbf{w}_i$  by quaternion QR algorithm.
- 26:    $f^{(t)} = \sum_{i=1}^{\ell} \|\mathbf{F}_i \mathbf{w}_t\|_s^s$ .
- 27:    $\mathbf{W} \leftarrow [\mathbf{W}, \mathbf{w}_t]$ .
- 28:    $\mathbf{D} = [\mathbf{D}, f^{(t)}]$ .
- 29:    $\mathbf{F}_i = \mathbf{F}_i^0 (\mathbf{I} - \mathbf{W}\mathbf{W}^*)$ ,  $i = 1, 2, \dots, \ell$ .
- 30: **end for**

---

Recall that  $\Psi$  is the average image of all training samples. Compute the projections of  $\ell$  training face images in the subspace  $\mathbf{W}$ ,

$$\mathbf{P}_s = (\mathbf{F}_s - \Psi) \mathbf{W} \in \mathbb{Q}^{m \times r}, \quad s = 1, \dots, \ell. \quad (4.1)$$

The columns of the matrix  $\mathbf{P}_s$ ,  $\mathbf{y}_t = (\mathbf{F}_s - \Psi) \mathbf{w}_t$ ,  $t = 1, \dots, r$ , are called the *principal component (vectors)* and  $\mathbf{P}_s$  is called the *feature matrix* or *feature image* of the sample image  $\mathbf{F}_s$ . Then in our experiment we use the 1-nearest neighbor (1NN) for the classification with the feature matrix. In Algorithm 2, we propose the procedure of G2DQPCA with weighted projection for image recognition.

---

**Algorithm 2 G2DQPCA with Weighted Projection for Image Classification**


---

- 1: For the mean-centered given training samples  $\mathbf{F}_s - \Psi$ ,  $s = 1, 2, \dots, \ell$ , compute the  $r$  ( $1 \leq r \leq n$ ) projection vectors and their corresponding weighted coefficient by Algorithm 1, denoted as  $(\mathbf{w}_1, f^{(1)}), \dots, (\mathbf{w}_r, f^{(r)})$ .
- 2: Let the eigenface subspace be  $\mathbf{W} = \text{span}\{f^{(1)}\mathbf{w}_1, \dots, f^{(r)}\mathbf{w}_r\}$ , where  $f^{(i)} = f^{(i)}/\text{sum}(f)$ .
- 3: Compute the projections of  $\ell$  training color face images in the subspace,  $\mathbf{W}$ ,

$$\mathbf{P}_s = (\mathbf{F}_s - \Psi)\mathbf{W} \in \mathbb{Q}^{m \times r}, \quad s = 1, \dots, \ell. \quad (4.2)$$

- 4: For a given testing sample,  $\mathbf{F}$ , compute its feature matrix,  $\mathbf{P} = (\mathbf{F} - \Psi)\mathbf{W}$ . Seek the nearest face image,  $\mathbf{F}_s$  ( $1 \leq s \leq \ell$ ), whose feature matrix satisfies that  $s = \text{argmin}\|\mathbf{P}_s - \mathbf{P}\|$ .  $\mathbf{F}_s$  is output as the person to be recognized.

---

We close this section by applying G2DQPCA to color image reconstruction. After obtaining the projection matrix, all we need is to project test image into eigenface space, i.e.

$$\mathbf{F}_s^{rec} = (\mathbf{F}_s - \Psi)\mathbf{W}\mathbf{W}^* + \Psi. \quad (4.3)$$

That is, we only use the first  $r$  projection vectors to reconstruct the original image. The important thing to note here is the process of reconstruction does not need to magnify the effect of features, so the projection matrix  $\mathbf{W}$  is unweighted. In Algorithm 3, we present the reconstructive process.

---

**Algorithm 3 G2DQPCA for Image Reconstruction**


---

- 1: For the mean-centered given training samples  $\mathbf{F}_s - \Psi$ ,  $s = 1, 2, \dots, \ell$ , compute the  $r$  ( $1 \leq r \leq n$ ) projection vectors by Algorithm 1, denoted as  $(\mathbf{w}_1, \mathbf{w}_2, \dots, \mathbf{w}_r)$ .
- 2: Let the eigenface subspace be  $\mathbf{W} = \text{span}\{\mathbf{w}_1, \dots, \mathbf{w}_r\}$ , and project a given testing sample  $\mathbf{F}$  into the space spanned by  $\mathbf{W}$ .
- 3: Adding the average image of all training samples,

$$\mathbf{F}^{rec} = (\mathbf{F} - \Psi)\mathbf{W}\mathbf{W}^* + \Psi \quad (4.4)$$

is output as the image to be reconstructed.

---

## 5 EXPERIMENTS

In this section, we evaluate the proposed G2DQPCA and WG2DQPCA models on three face databases:

- GTFD—The Georgia Tech Face Database(GTFD) [47] contains 750 images from 50 subjects, fifth images per subject. It includes various pose faces with various expressions on cluttered backgrounds. All the images are manually cropped, and then resized to  $44 \times 33$  pixels. Some cropped images occluded with noise are shown in Figure 5.1.
- Color Feret—The color FERET database [48] contains 1199 persons, 14126 color face images, and each person has various numbers of face images with various backgrounds. The minimal number of face images for one person is 6, and the maximal one is 44.

The size of each cropped color face image is  $192 \times 128$  pixels. Here we take 11 images of 275 individuals as an example. Some samples occluded with noise are shown in Figure 5.2.

- Faces95—Faces95 database [49] contains 1440 images photographed over a uniform background from 72 subjects, 20 images per subject. The size of each color face image is  $200 \times 180$  pixels. Some samples are displayed in Figure 5.3.

The numerical experiments are to test the efficiencies of the methods in the task of image reconstruction and classification with or without noise.

**Example 5.1** (Face Recognition with Clean Training Data). *We firstly proceed to investigate the classification performance of G2DQPCA and WG2DQPCA on all three databases with clean training data. We randomly select 90 percent of data set as training set and the remaining as the testing set. Of course, training set is guaranteed to contain at least one image of each individual. The whole procedure is repeated three times and the average recognition rate is reported.*

*In Figures 5.4, 5.5 and 5.6, we present the classification accuracies of G2DQPCA and WG2DQPCA methods applied on three face databases in different cases. Note that when  $s = 2, p = 2$ , G2DQPCA reduces to 2DQPCA [1]. For simplicity, let  $(s, p)$  denote G2DQPCA with  $L_s$ -norm and  $L_p$ -norm, and  $w(s, p)$  WG2DQPCA with  $L_s$ -norm and  $L_p$ -norm in all figures. We find that the classification accuracies of WG2DQPCA are much higher than those of G2DQPCA. The results indicate that the recognition rate of G2DQPCA decreases as the number of features increases, but the recognition rate of WG2DQPCA remains unchanged or perturbs tightly. Also, we can find that different databases have different optimal parameter pair  $w(s, p)$ . For the GTFD, Color Feret, and Faces95 databases, the optimal recognition rates are reached when  $w(s = 1, p = 2)$ ,  $w(s = 2, p = 2)$  and  $w(s = 2, p = \infty)$ , respectively.*

**Example 5.2** (Face Recognition with Noisy Training Data). *We examine the recognition performance of G2DQPCA and WG2DQPCA with polluted training set while the testing set are clean. On three databases, two different noises are considered separately. In the first case, the noise consists of random black and white dots. We randomly added this noise to 20% of the training set. The location of noise is arbitrary, and the size is at least  $10 \times 10$ . The second case is to add salt and pepper noise to the training set. Here we set the noise density as 0.02, 0.05 and 0.1, respectively.*

*Same as before, the whole procedure of each case is repeated three times. Figures 5.7, 5.8 and 5.9 show the average classification accuracy with different occluded training set on three databases. In general, the results indicate that a polluted training set will impact the classification performance, because the feature extraction is affected by noise. However, we can still find that recognition rate of WG2DQPCA is more stable and higher than that of G2DQPCA. Obviously, under the influence of different noises, the optimal parameter pair  $w(s, p)$  is not fixed for each database. Figure 5.7 shows that for GTFD database, WG2DQPCA with  $s = 2$  and  $p = 2$  has good performance in the case of black and white dots noise, WG2DQPCA with  $s = 1$  and  $p = \infty$  works well when the salt and pepper noise density are 0.02 and 0.05, and WG2DQPCA with  $s = 1$  and  $p = 2$  performs*



Fig. 5.1: Sample images with or without occlusion of the Georgia Tech face database.



Fig. 5.2: Some samples with or without occlusion of one person from the Color Feret database.

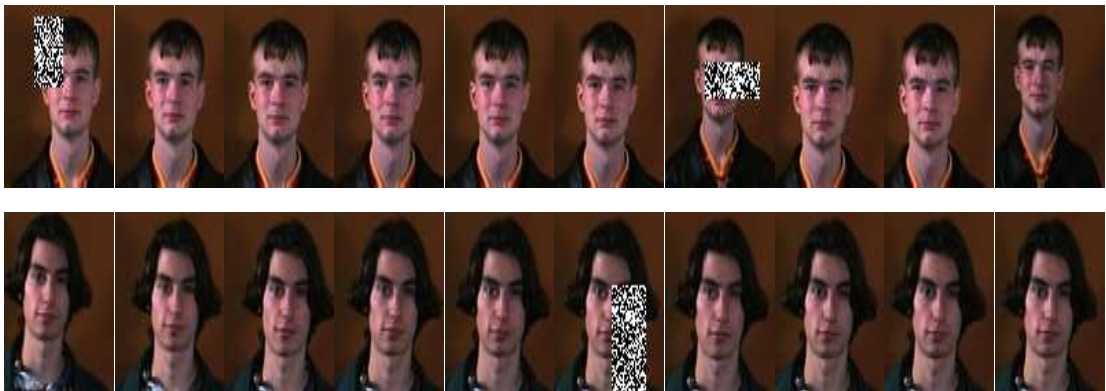


Fig. 5.3: Some samples with or without occlusion of one person from the Faces95 database.

better in the last case. For Faces95 database, Figure 5.8 indicates that WG2DQPCA with  $s = 2$  and  $p = \infty$  achieves the highest classification accuracy in all cases. As for Color Feret database, we can observe that the performance of WG2DQPCA with  $s = 2$  and  $p = 2$  is relatively stable from Figure 5.9.

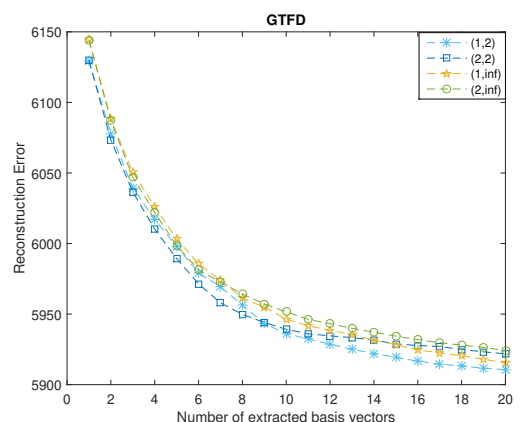


Fig. 5.10: Reconstruction errors of G2DQPCA on the GTFD database.

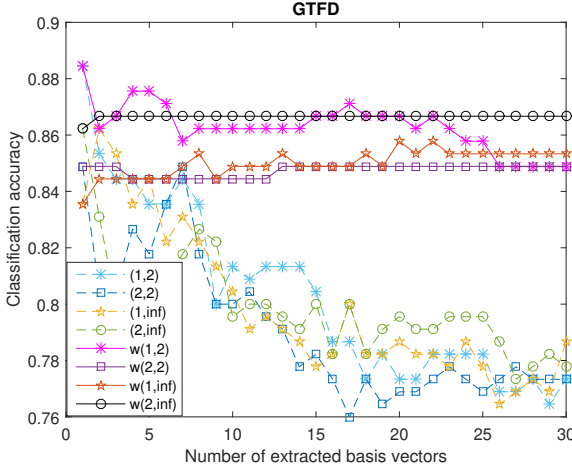


Fig. 5.4: Classification accuracies of G2DQPCA and WG2DQPCA, denoted by  $(s, p)$  and  $w(s, p)$ , respectively, on the GTFD database.

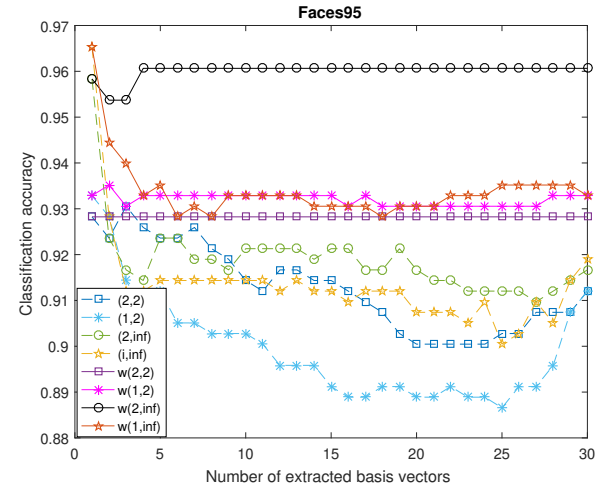


Fig. 5.6: Classification accuracies of G2DQPCA and WG2DQPCA on the Faces95 database.

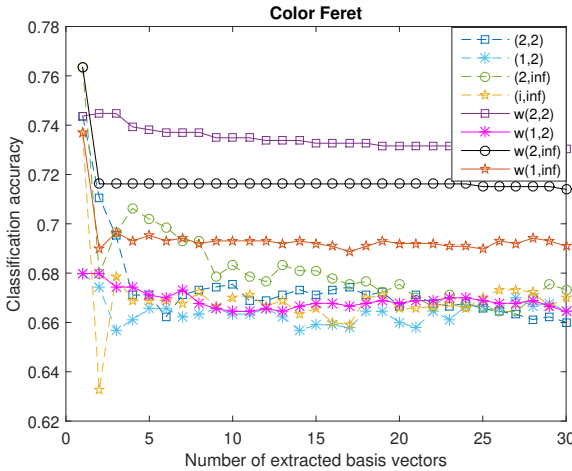


Fig. 5.5: Classification accuracies of G2DQPCA and WG2DQPCA on the Color FERET database.

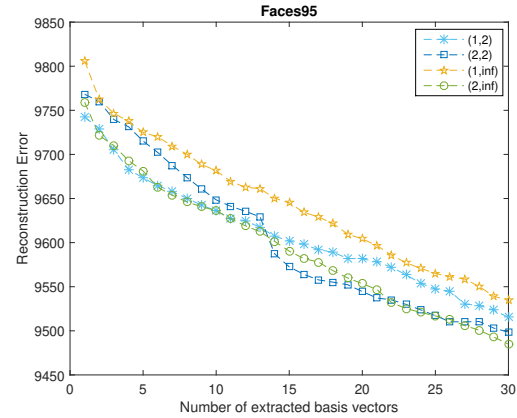


Fig. 5.12: Reconstruction errors of G2DQPCA on the Faces95 database.

**Example 5.3 (Color Image Reconstruction).** Finally, we evaluate the reconstruction performance of G2DQPCA algorithm. Here 20% of the three databases have randomly selected to add black and white dots noise, respectively.

The following reconstruction error is used to measure the quality of methods:

$$err = \frac{1}{\ell} \sum_{i=1}^{\ell} \|\mathbf{F}_i^{clean}(\mathbf{I} - \mathbf{W}\mathbf{W}^*)\|_F \quad (5.1)$$

where  $\ell$  is the number of clean training data,  $\mathbf{F}_i^{clean}$  is the  $i$ -th clean training sample and  $\mathbf{W}$  is the projection matrix trained on the whole polluted training database. As emphasized in Section 4,  $\mathbf{W}$  is unweighted here because the process of reconstruction does not need to magnify the effect of features.

Figure 5.10 shows the reconstruction errors of G2DQPCA in several special cases with the number of features from 1 to 20 on GTFD database. Figures 5.11 and 5.12 show the reconstruction errors of G2DQPCA with the feature number from 1 to 30 on the other two databases. From the results, all parameter pairs are indicated to have a good performance in image reconstruction. With the increase of features number, we find that applying  $L_1$ -norm on the objective function, i.e.,  $s = 1, p = 2$ , is effective for the images reconstruction on GTFD database and Color Feret

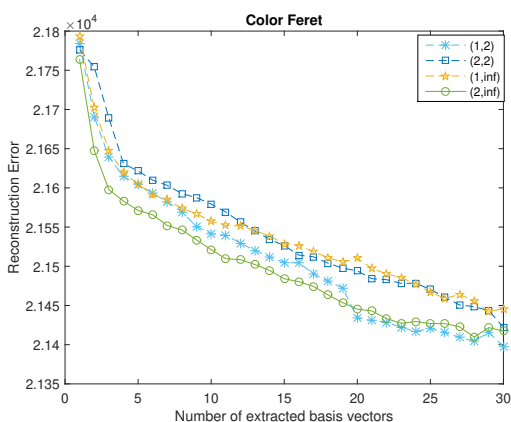


Fig. 5.11: Reconstruction errors of G2DQPCA on the Color Feret database.

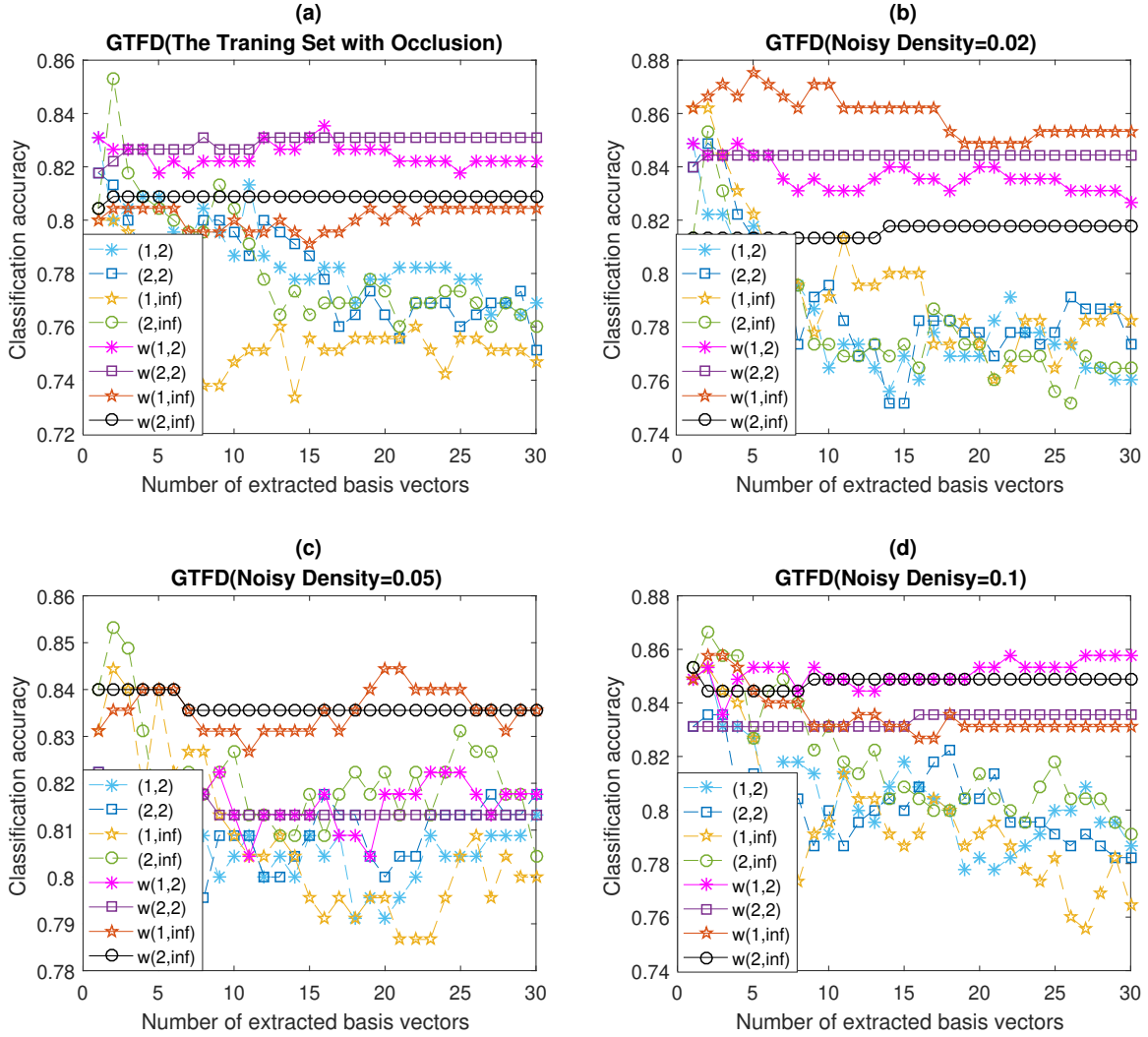


Fig. 5.7: Classification accuracies with polluted training set of G2DQPCA and WG2DQPCA on the GTFD database. (a) The training set with black and white dots noise. (b)-(d) The training set with Salt and Pepper Noise where the noise density are 0.02, 0.05 and 0.1, respectively.

database. G2DQPCA works well on the Faces95 database when  $s = 2, p = 2$  and  $s = 2, p = \infty$ . As an illustration, Figures 5.13, 5.14 and 5.15 show some reconstructed images.

## 6 CONCLUSION

The proposed G2DQPCA model is a generalization of 2DQPCA with applying  $L_p$ -norm both in the objective function and the constraint function. An iterative algorithm under the MM framework on quaternion domain is designed to solve the optimization problem of G2DQPCA and a closed-form solution is obtained at each step of iteration. Besides, the quaternion QR algorithm is used to ensure the orthogonality of the computed projection bases. G2DQPCA with weighted projection (WG2DQPCA) is further presented to enhance the role of main features for face recognition. The numerical experiments indicate that WG2DQPCA has a higher and more stable face recognition rate than state of-the-art methods. In addition, G2DQPCA is also effective in image reconstruction.

## REFERENCES

- [1] Z.-G. Jia, S.-T. Ling and M.-X. Zhao, *Color two-dimensional principal component analysis for face recognition based on quaternion model*, LNCS, 10361 (2017) 177-189.
- [2] M. Zhao, Z. Jia and D. Gong, *Improved Two-Dimensional Quaternion Principal Component Analysis*, IEEE Access, 7 (2019) 79409-79417.
- [3] X. Xiao and Y. Zhou, *Two-Dimensional Quaternion PCA and Sparse PCA*, IEEE Transactions on Neural Networks and Learning Systems, 30(7) (2019) 2028-2042.
- [4] X. Xiao, Y. Chen, Y. Gong and Y. Zhou, *2D Quaternion Sparse Discriminant Analysis*, IEEE Trans. Image Process., 29(1) (2020) 2271-2286.
- [5] M. Zhao, Z. Jia, Y. Cai, X. Chen and D. Gong *Advanced Variations of two-dimensional principal component analysis for face recognition*, Neurocomputing, accepted.
- [6] J. Yang, D. Zhang, A. F. Frangi, and J. Y. Yang, *Two-dimensional PCA: A new approach to appearance-based face representation and recognition*, IEEE Trans. Pattern Anal. Mach. Intell., 26(1) (2004) 131-137.
- [7] M. A. Turk and A. P. Pentland, *Face recognition using eigenfaces*, Proc. IEEE Conf. Comput. Vis. Pattern Recognit., (1991) 586-591.
- [8] Q. Ke and T. Kanade, *Robust  $L_1$  norm factorization in the presence of outliers and missing data by alternative convex programming*, IEEE Conf. Comput. Vis. Pattern Recognit., San Diego, CA, USA, 2005, 739-746.

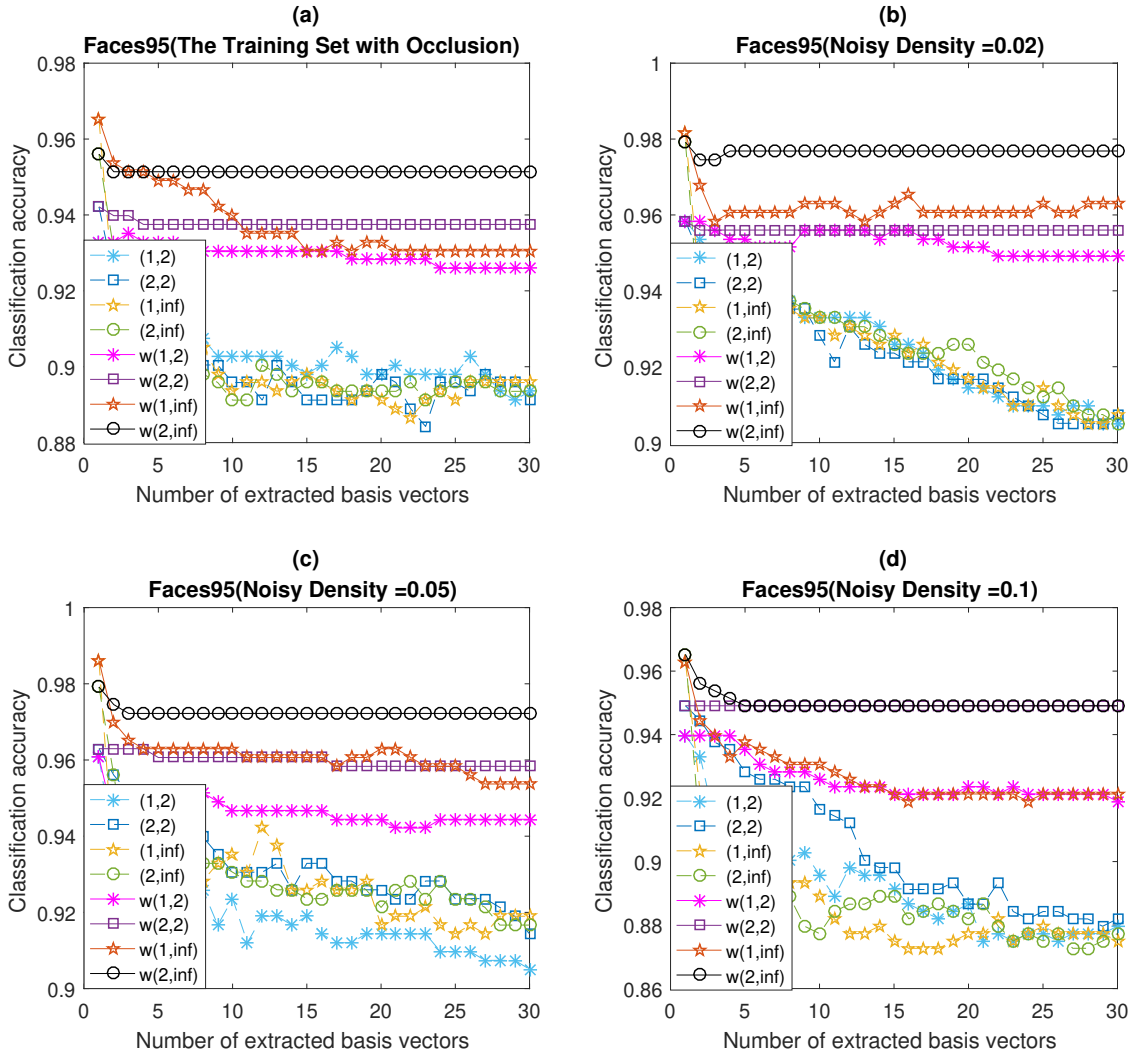


Fig. 5.8: Classification accuracies with polluted training set of G2DQPCA and WG2DQPCA on the Faces95 database. (a) The training set with black and white dots noise. (b)-(d) The training set with Salt and Pepper Noise where the noise density are 0.02, 0.05 and 0.1, respectively.

- [9] C. Ding, D. Zhou, X. He, and H. Zha, *R<sub>1</sub>-PCA: Rotational invariant L<sub>1</sub>-norm principal component analysis for robust subspace factorization*, Proc. Int. Conf. Machine Learning (ICML 2006), (2006) 281-288.
- [10] N. Kwak, *Principal component analysis based on L<sub>1</sub>-norm maximization*, IEEE Trans. Pattern Anal. Mach. Intell., 30 (9) (2008) 1672-1680.
- [11] S. Boyd and L. Vandenberghe, *Convex Optimization*, Cambridge university press, 2009.
- [12] H. Zou and T. Hastie, *Regularization and variable selection via the elastic net*, Journal of the Royal Statistical Society: Series B (Statistical Methodology), 67(2) (2005) 301-320.
- [13] H. Zou, T. Hastie and R. Tibshirani, *Sparse principal component analysis*, J. Comput. Graph. Stat., 15(2) (2006) 265-286.
- [14] H. Shen and J. Z. Huang, *Sparse principal component analysis via regularized low rank matrix approximation*, J. Multivar. Anal., 99(6) (2008) 1015-1034.
- [15] M. Journée, Y. Nesterov, P. Richtárik, and R. Sepulchre, *Generalized power method for sparse principal component analysis*, The Journal of Machine Learning Research, 11 (2010) 517-553.
- [16] F. R. On, R. Jailani, S. L. Hassan and N. M. Tahir, *Analysis of sparse PCA using high dimensional data*, 2016 IEEE 12th International Colloquium on Signal Processing & Its Applications (CSPA2016), (2016) 340-345.
- [17] M. I. Razzak, R. A. Saris, M. Blumenstein and G. Xu, *Robust 2D Joint Sparse Principal Component Analysis With F-Norm Minimization For Sparse Modelling: 2D-RJSPCA*, International Joint Conference on Neural Networks (IJCNN), (2018) 1-7.
- [18] D. Meng, Q. Zhao, and Z. Xu, *Improve robustness of sparse PCA by L<sub>1</sub>-norm maximization*, Pattern Recognit., 45 (1) (2012) 487-497.
- [19] P. Peng, Y. Zhang, F. Liu, H. Wang and H. Zhang, *A Robust and Sparse Process Fault Detection Method Based on RSPCA*, IEEE Access, 7 (2019) 133799-133811.
- [20] Z. Liang, S. Xia, Y. Zhou, L. Zhang, and Y. Li, *Feature extraction based on L<sub>p</sub>-norm generalized principal component analysis*, Pattern Recognit. Lett., 34(9) (2013) 1037-1045.
- [21] N. Kwak, *Principal component analysis by L<sub>p</sub>-norm maximization*, IEEE Trans. Cybern., 44(5) (2014) 594-609.
- [22] J. Ye, *Generalized low rank approximations of matrices*, Mach. Learn., 61 (2005) 167-191.
- [23] D. Zhang and Z.-H. Zhou, *(2D)<sup>2</sup>PCA: Two-directional twodimensional PCA for efficient face representation and recognition*, Neurocomputing, 69(1) (2005) 224-231.
- [24] X. Li, Y. Pang, and Y. Yuan, *L<sub>1</sub>-norm-based 2DPCA*, IEEE Trans. Syst. Man, Cybern. B, Cybern., 40 (4) (2010) 1170-1175.
- [25] J. Meng and X. Zheng, *Robust Sparse 2DPCA and Its Application to Face Recognition*, Symposium on Photonics and Optoelectronics, (2012) 1-4.
- [26] J. Wang, *Generalized 2-D Principal Component Analysis by L<sub>p</sub>-Norm for Image Analysis*, IEEE transactions on cybernetics, 46(3) (2016) 792-803.

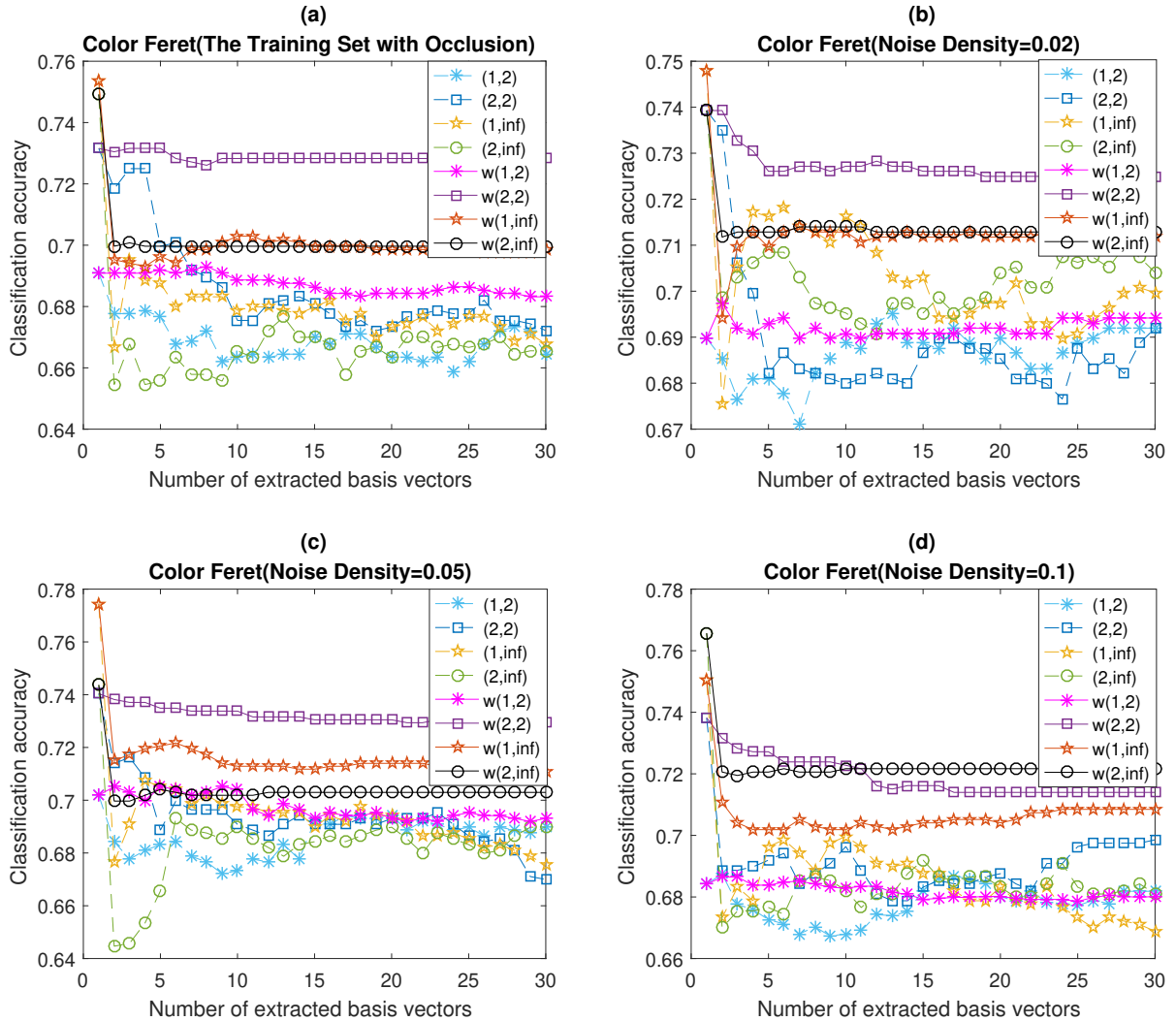


Fig. 5.9: Classification accuracies with polluted training set of G2DQPCA and WG2DQPCA on the Color Feret database. **(a)** The training set with black and white dots noise. **(b)-(d)** The training set with Salt and Pepper Noise where the noise density are 0.02, 0.05 and 0.1, respectively.



Fig. 5.13: The reconstructed images of G2DQPCA on two sample images from the polluted GTFD database. The first column are the images to be reconstructed. The following three columns are the reconstructed images by using the first 20 projection vectors of G2DQPCA wherein the  $(s, p)$  pairs are set to be  $(1, 2)$ ,  $(2, 2)$  and  $(2, 1)$  in order. The last column shows the original images for comparison.

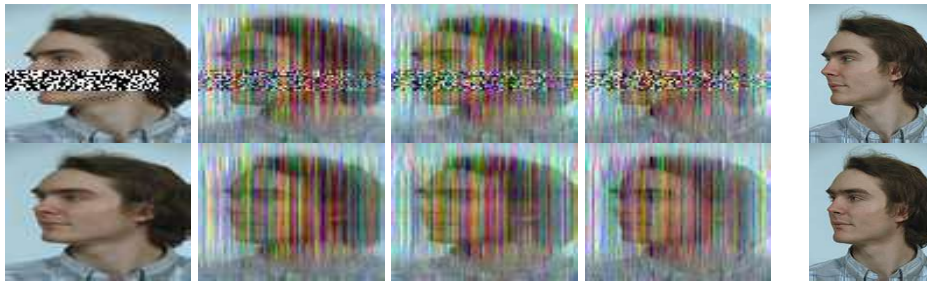


Fig. 5.14: The reconstructed images of G2DQPCA on two sample images from the polluted color Feret database. The first column are the images to be reconstructed. The following three columns are the reconstructed images by using the first 20 projection vectors of G2DQPCA wherein the  $(s, p)$  pairs are set to be  $(1, 2)$ ,  $(2, 2)$  and  $(2, 1)$  in order. The last column shows the original images for comparison.

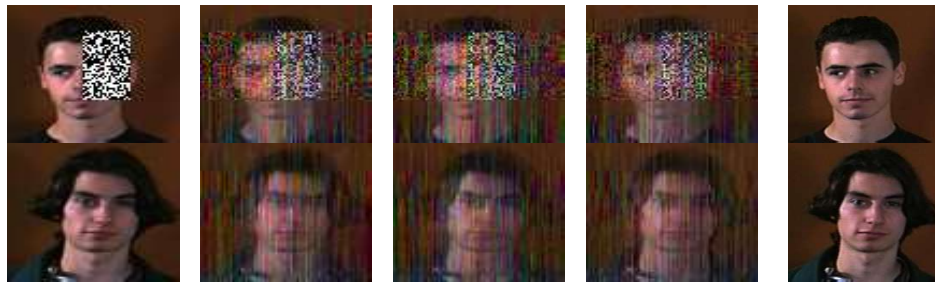


Fig. 5.15: The reconstructed images of G2DQPCA on two sample images from the polluted Faces95 database. The first column are the images to be reconstructed. The following three columns are the reconstructed images by using the first 20 projection vectors of G2DQPCA wherein the  $(s, p)$  pairs are set to be  $(1, 2)$ ,  $(2, 2)$  and  $(2, 1)$  in order. The last column shows the original images for comparison.

- [27] X. Chen, Z.-G. Jia, Y.-F. Cai and M.-X. Zhao, *Relaxed 2-D Principal Component Analysis by  $L_p$  Norm for Face Recognition*, arXiv e-prints, (2019) arXiv:1905.06458.
- [28] J. Mairal, M. Elad, and G. Sapiro, *Sparse representation for color image restoration*, IEEE Trans. Image Process., 17(1) (2008) 53-69.
- [29] R. Lan and Y. Zhou, *Quaternion-michelson descriptor for color image classification*, IEEE Trans. Image Process., 25(11) (2016) 5281-5292.
- [30] X. Xiang, J. Yang, and Q. Chen, *Color face recognition by PCA-like approach*, Neurocomputing, 152 (2015) 231-235.
- [31] C. Zou, K. I. Kou and Y. Wang, *Quaternion Collaborative and Sparse Representation With Application to Color Face Recognition*, IEEE Trans. Image Process. 25(7) (2016) 3287-3302.
- [32] N. L. Bihan and S. J. Sangwine, *Quaternion principal component analysis of color images*, Proc. 2003 Tenth IEEE Int. Conf. Image Processing (ICIP 2003), 1 (2003) 809-812.
- [33] Y. F. Sun, S. Y. Chen and B. C. Yin, *Color face recognition based on quaternion matrix representation*, Pattern Recognit. Lett., 32(4) (2011) 597-605.
- [34] B. J. Chen, J. H. Yang, B. Jeon and X. P. Zhang, *Kernel quaternion principal component analysis and its application in RGB-D object recognition*, Neurocomputing, 266(29) (2017) 293-303.
- [35] J. Ye and Q. Li, *A two-stage linear discriminant analysis via QR decomposition*, IEEE Trans. Pattern Anal. Mach. Intell., 27(6) (2005) 929-941.
- [36] S. Noushath, G. Hemantha Kumar and P. Shivakumara,  *$(2D)^2$ LDA: An efficient approach for face recognition*, Pattern Recognition, 39(7) (2006) 1396-1400.
- [37] Z. Liang, Y. Li and P. Shi, *A note on two-dimensional linear discriminant analysis*, Pattern Recognition Letters, 29(16) (2008) 2122-2128.
- [38] Z.-G. Jia, M. K. Ng and G.-J. Song, *Lanczos method for large-scale quaternion singular value decomposition*, Numer. Algor. 82(2) (2019) 699-717.
- [39] Z.-G. Jia, M. K. Ng and G.-J. Song, *Robust quaternion matrix completion with applications to image inpainting*, Numerical Linear Algebra with Applications, 26(4) (2019) e2245.
- [40] Z.-G. Jia, M. K. Ng and W. Wang, *Color image restoration by saturation-value total variation*, SIAM J. Imaging Sci., 12(2) (2019) 972-1000.
- [41] Y. Chen, X. Xiao and Y. Zhou, *Low-Rank Quaternion Approximation for Color Image Processing*, IEEE Trans. Image Process. 29(1) (2020) 1426-1439.
- [42] D. R. Hunter and K. Lange, *A tutorial on MM algorithms*, The American Statistician, 58(1) (2004) 30-37.
- [43] S. C. Pei and C. M. Cheng, *Quaternion matrix singular value decomposition and its applications for color image processing*, Proc. 2003 Int. Conf. Image Processing (ICIP 2003), 1 (2003) 805-808.
- [44] Z. Jia, M. Wei, S. Ling, *A new structure-preserving method for quaternion Hermitian eigenvalue problems*, J. Comput. Appl. Math. 239(2013) 12-24.
- [45] Z.-G. Jia, M. Wei, M.-X. Zhao and Y. Chen, *A New Real Structure-preserving Quaternion QR Algorithm*, Journal of Computational and Applied Mathematics, 343 (2018) 26-48.
- [46] W. H. Yang, *On generalized Hölder inequality*, Nonlinear Analysis: Theory, Methods & Applications, 16(5) (1991) 489-498.
- [47] The Georgia Tech face database: [http://www.anefian.com/research/face\\_reco.htm](http://www.anefian.com/research/face_reco.htm).
- [48] The color FERET database: <https://www.nist.gov/itl/iad/image-group/color-feret-database>.
- [49] The Faces95 database: <https://cswww.essex.ac.uk/mv/allfaces/faces95.html>.